E. WOLF, PROGRESS IN OPTICS XII © NORTH-HOLLAND 1974

IV

INTERACTION OF LIGHT WITH MONOMOLECULAR DYE LAYERS

BY

KARL H. DREXHAGE*

Physikalisch-Chemisches Institut der Universität, Marburg/Lahn, Germany

* Now with Eastman Kodak Research Laboratories, Rochester, N.Y., USA.

CONTENTS

§ 1. Introduction

Although light is the most familiar form of electromagnetic radiation, some aspects of its generation and propagation have not been as carefully studied as the corresponding behavior of microwaves or radio waves. The reason for this can be traced to the short wavelength of light, which is small compared with the dimensions of most physical apparatus. Recently a new investigative technique has become available that avoids the difficulties traditionally associated with the short wavelength of light.

This development was initiated by ZWICK and KUHN [1962], who were looking for a novel method of studying experimentally the distance dependence of energy transfer from an excited donor molecule to a nearby acceptor molecule. The idea was to separate physically donor and acceptor by a well defined distance and then to examine the fluorescence of donor or acceptor as a function of separation. They attempted this with layers of adsorbed dyes separated by means of monomolecular fatty acid layers, as was first suggested by AUGENSTINE [1960]. Stimulated by these experiments, F. P. Schäfer suggested the possibility of using monomolecular layers of fluorescent dyes to study *optical* phenomena such as standing light waves and the influence of a mirror on the light emission by molecules. After an improved monolayer technique had become available, these ideas were realized experimentally (DREXHAGE [1966], BÜCHER, DREXHAGE, FLECK, KUHN, MÖBIUS, SCHÄFER, SONDERMANN, SPERLING, TILLMANN, WIEGAND [1967]).

The new technique has found a great variety of applications other than in optics, which have been reviewed recently by KUHN and MÖBIUS [1971], KUHN [1972] and MÖBIUS and BÜCHER [1972]. In this article we shall concentrate on the optical studies, emphasizing those phenomena that have been examined for the first time. We shall begin by describing the preparation of monolayer systems and the determination of their optical constants. The experiments with dye layers which are reviewed in the later sections may be divided into two classes: (1) The dye acts as a weakly absorbing probe for the light field and its light emission (fluorescence) serves merely as a measure thereof. (2) The absorption of light by the dye only provides the energy for

the fluorescence, which is the phenomenon to be examined. Clearly, the two situations are reciprocal, and often both types of experiments can be made with the same sample.

§ 2. Preparation of Monolayer Systems

The technique of built-up films on which the work to be discussed in this article is based, was founded by BLODGETT [1934, 1935] and BLODGETT and LANGMUIR [1937]. An important improvement was introduced by SHER and CHANLEY [1955], who replaced the "piston oil" used by Blodgett and Langmuir for the compression of the film, by a floating barrier. For general reviews of the monolayer technique the reader is referred to TRURNIT [1945], GAINES [1966] and MÖBIUS and BÜCHER [1972]. In this section we summarize the preparation of built-up films from fatty-acid and dye monolayers only insofar as it is relevant to the work dealt with in the subsequent sections of this article.

2.1. DEPOSITION OF CADMIUM–ARACHIDATE LAYERS

When a solution of a long-chain fatty acid, e.g. arachidic acid ($C_{19}H_{39}COOH$), in an organic solvent like benzene or chloroform is dropped onto a clean water surface, the solvent evaporates quickly and leaves the arachidic acid, which is insoluble in water, at the surface. The fatty-acid molecules are attached to the water with the hydrophilic carboxyl group, whereas the other end of the molecule is hydrophobic and tends to point upward. Depending on the surface area and the concentration of the arachidic-acid solution one has to add a certain number of drops to the water surface in order to cover it completely with a monomolecular film of the acid. This

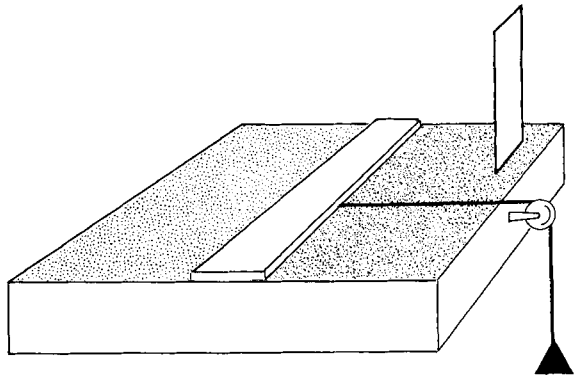

Fig. 1. Deposition of monomolecular layers with the Blodgett technique.

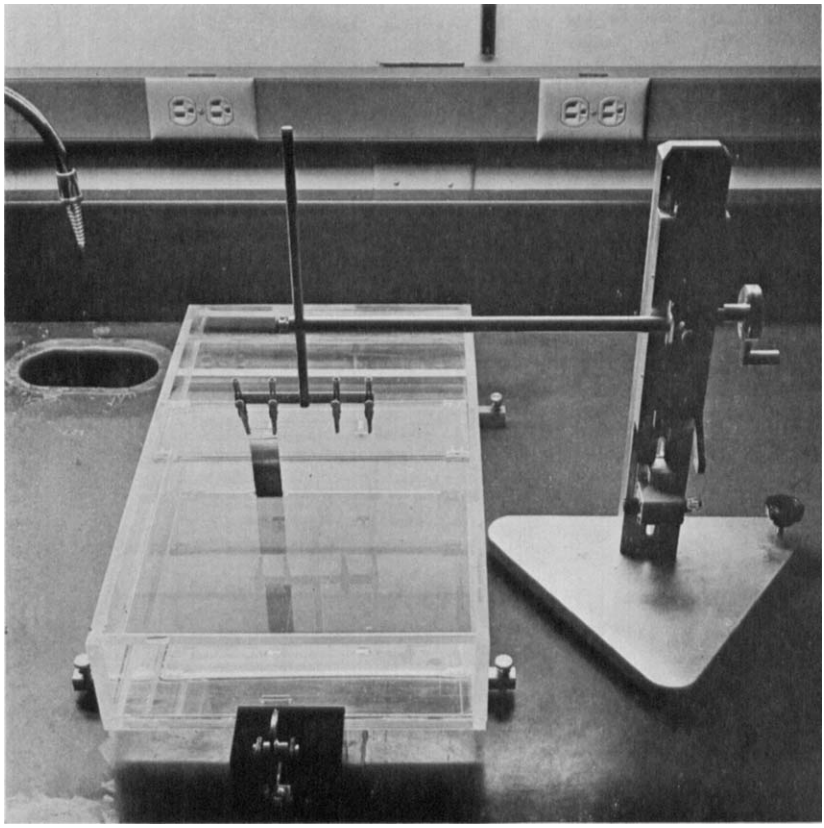

Fig. 2. Apparatus used by the author to deposit monomolecular layers on a glass slide. The trough and floating barrier are made from plexiglass. The trough is 30 cm wide, 60 cm long and 8 cm deep. The width of the float (length 8 cm) is by about 2 mm smaller than the inside of the trough. The sides of the float as well as the rim of the trough are polished and parallel to allow a smooth, piston-like movement. The adjustable stop at the bottom of the dipping device carries a counter. (From DREXHAGE [1970b], used with permission of Scientific American.)

point is easy to perceive since the drops no longer spread, but remain unchanged in form of small lenses floating on the surface. The solvent would evaporate slowly from these droplets and leave the acid behind in crystalline form. This is avoided, however, by moving a float backwards (Figs. 1 and 2), so that the surface area available to the fatty-acid film is increased and the droplets spread immediately. By means of a weight-and-pulley arrangement (Fig. 1) one now applies a small force to the float, in order to exert a surface pressure on the film. Under the pressure the arachidic–acid molecules form a densely packed monomolecular film covering the water surface in front of

the float, the thickness of which is equal to the length of the arachidic–acid molecules.

For preparation purposes the film is kept under a surface pressure of about 30 dyne/cm corresponding to a weight of about 1 g per 30 cm float width. As the arachidic–acid film is nearly incompressible between 5 and 60 dyne/cm, small pressure changes, which may occur during the preparation process, do not affect the packing of the molecules in the film. Under the right conditions (see below) the film can be transferred to almost any substrate. If, for instance, a glass plate is lowered through the surface, on withdrawal one layer of arachidic acid is deposited on the hydrophilic glass. The carboxylic end groups of the arachidic acid attach themselves to the glass surface (Fig. 3), and the slide emerges dry from the water. Because the terminal CH_3-groups of the arachidic acid point outward, the surface of

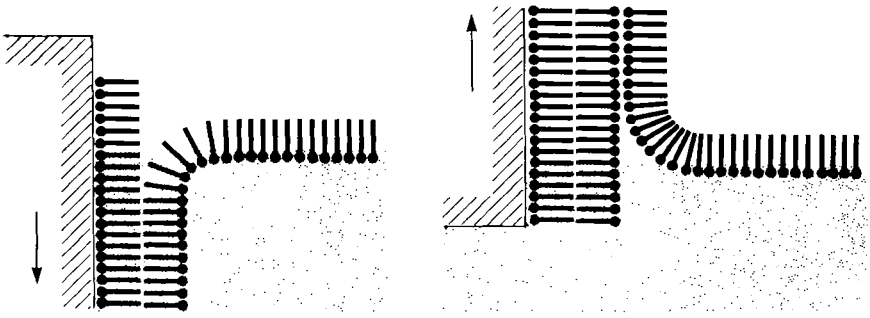

Fig. 3. Schematic picture of the molecular arrangement in perfect CdC_{20} layer-systems.

the slide is now hydrophobic, and on the next dipping *two* additional layers are deposited. This process may be repeated many times until the layer system has the desired thickness, which is given by the number of deposited arachidic-acid layers times the thickness of a single layer. The deposition of the monolayer can be monitored by watching the float moving forward under the influence of the weight as the film is removed from the water surface. When the film has been used up, the float is removed and a hydrophobic barrier is moved across the surface of the water. Thereby the remainder of the film is pushed toward the rear end of the trough, where it can be removed by a strip of filter paper, and the main area of the water surface is now clean again and can be covered with a fresh monomolecular film.

The deposition of fatty-acid layers is aided by the presence of bivalent metal ions in the water upon which the film is formed. Thereby the fatty acid is converted into its salt to a degree which depends on the ion concen-

tration and the p_H-value of the water. Barium chloride and stearic acid ($C_{17}H_{35}COOH$) have been most often used to build monolayer systems (BLODGETT [1935]). The work we are concerned with in this article, however, has been done almost exclusively with monolayers of arachidic acid ($C_{19}H_{39}COOH$) formed on water which contains cadmium chloride. Although the technique appears to be very simple, the successful preparation of monolayer systems depends on a number of peculiarities of method that are not self-evident. Thus it may be worthwhile to consider here some important details of the preparation of cadmium-arachidate layers (DREXHAGE [1966]).

The experimental set-up used successfully by the author is shown in Fig. 2. After thorough cleaning of the trough it is filled to the brim with distilled (once is enough) water, and about one gram of cadmium chloride ($CdCl_2 \cdot 2.5\ H_2O$; analytical grade) is dissolved in the water, in order to obtain a cadmium-ion concentration of about 5×10^{-4} molar. With this concentration cadmium-arachidate (abbrev.: CdC_{20}) layers are best deposited at a p_H-value of about 5.5, which coincides with the acidity of air-saturated water and therefore maintains itself automatically, and no buffering or other additives to the water are called for. By comparison, barium–stearate layers are best deposited at a p_H-value of 8.5 (BLODGETT [1935]), which is more difficult to keep constant due to the continuous absorption of carbon dioxide from the air. The good optical quality of cadmium-arachidate layers was already noticed by BLODGETT [1939], and the writer found them superior to fatty-acid monolayers formed on water that contained Ba^{2+}, Sr^{2+}, Ca^{2+}, Mn^{2+}, Co^{2+} or Zn^{2+}-ions at various concentrations.

The arachidic acid is applied to the water surface from a solution containing ~1.5 mg per ml of solvent. If the concentration is too high, evaporation produces saturation before the monomolecular film is fully developed, so that some crystalline arachidic acid is left behind, contaminating the film. On the other hand, a much smaller concentration of arachidic acid is not recommended, because a large quantity of solvent has to be transferred to the surface. Thus an unnecessarily large amount of non-volatile impurities present in the solvent is incorporated into the film. It is advisable to use only purified solvents that evaporate without any noticeable residue, which is usually the case after a thorough distillation over a column. The arachidic-acid solution should be handled only with extremely clean, surfactant-free glassware, the cleanliness of which can be ensured by rinsing it before use with distilled chloroform. Any contact of the solution with materials like rubber, cork, plastics etc. is to be avoided. Because chloroform attacks plexiglass, some caution is required on application of the solution to the surface. A watch-glass on the bottom of the trough catches droplets that may fall through the water surface.

The most serious problem encountered in the preparation of high-quality layers concerns the purity of the arachidic acid, because any impurities invariably become incorporated into the film and may ruin its homogeneity. Arachidic-acid samples that are commercially available, are often not sufficiently pure, even if labeled "purissimum"*. This usually causes a foggy appearance of layer systems with more than about 50 CdC_{20} monolayers, and the glass plates tend to emerge wet from the trough, after about 100 CdC_{20} monolayers have been deposited. With pure arachidic acid, however, the plates emerge entirely dry even after deposition of more than 500 monolayers, and scattering of light is almost

* The author expresses his gratitude to Dr. H. Lange, Henkel and Cie. GmbH, Düsseldorf, Germany for a valuable gift of highly pure arachidic acid. – Recently arachidic acid of good quality has become available from Analabs, Inc., North Haven, Connecticut.

undetectable by the naked eye. Although the quality of such layers can be considered excellent for many applications, it is still by far inferior to the optical quality of thin films prepared by modern evaporation techniques.

Before the actual film deposition begins, the surface is covered with a scavenging arachidic-acid film. Impurities in the trough solution that would otherwise contaminate the operational film enter the scavenging film and are swept away upon its removal. After scavenging has been repeated several times, the trough solution can be considered clean and is now ready for reproducible film deposition. The same solution can be used unchanged for several weeks.

The microscope slides to be used as substrates for the monolayer systems are cleaned preferably with an ultrasonic cleaner containing an alkaline cleansing agent. Without an alkaline treatment, most glasses tend to shed the cadmium-arachidate layers after a few dippings. Subsequently the slides are rinsed thoroughly with distilled water and dried in a stream of hot air. Multilayer deposition on the hydrophilic glass surface yields an odd number of layers. Evaporated gold or silver films on glass are hydrophobic, and consequently an even-numbered set of monolayers is obtained.

It is advisable to watch closely the behavior of the meniscus at the glass surface during the dipping, which is preferably done *manually* with an apparatus like the one shown in Fig. 2. In case the operator observes any irregularities, he can stop the deposition at any moment. The dipping speed is not critical and is typically 10 cm/min; only the first monolayer may require more time for dry deposition. To ensure reproducible results, a film that has been sitting more than about five minutes on the trough solution should be replaced by a fresh one. In this way, the accumulation of dust particles from the atmosphere is kept at a negligible level.

A more refined deposition technique for CdC_{20} and other monolayers has been reported by BÜCHER, ELSNER, MÖBIUS, TILLMANN, WIEGAND [1969] (see also MÖBIUS and BÜCHER [1972]), in which a novel trough construction is used. The surface of the water is cleaned by sucking the film from the surface with an aspirator, and the $CdCl_2$ solution lost during this procedure is automatically replenished from a reservoir. In addition, the surface pressure is monitored during the deposition process, which can be helpful with monolayers whose properties depend sensitively on the surface pressure. For the deposition of cadmium-arachidate layers, however, this apparatus is unnecessarily sophisticated.

2.2. PREPARATION OF MONOMOLECULAR DYE LAYERS

The cadmium-arachidate layers, which are transparent in the visible and near ultraviolet part of the spectrum, serve in the work of this article as spacers to separate dye layers from each other or from metal mirrors or dielectric interfaces. Various types of thin layers of fluorescent dyes have been employed in studies of optical phenomena by several authors, e.g., DRUDE and NERNST [1892], SELÉNYI [1911, 1938], FREED and WEISSMAN [1941], SHKLYAREVSKII, MILOSLAVSKII, GOLOYADOVA [1964], KOSSEL [1958]. In most of this work the resolution was limited by the thickness of the dye layer, which was only slightly smaller than the wavelength of light. For a

higher precision this thickness would have to be reduced with the ultimate goal of a dye layer of molecular cross section, i.e. a monomolecular layer.

The first attempt to prepare such monomolecular layers of fluorescent dyes was reported by ZWICK and KUHN [1962]. They observed that certain dyes were adsorbed, when a glass plate coated with barium–stearate layers was immersed into an aqueous solution of the dye. This technique was applicable to many dyes, mostly of the cyanine type, and from the light absorption it was concluded that the amount of adsorbed dye corresponded in many cases roughly to a monolayer coverage (DREXHAGE, ZWICK, KUHN [1963], DREXHAGE [1964]). However, the dye layers, prepared by this technique, were not truly monomolecular in the sense that all dye molecules are located at the same clearly defined distance from the surface. Some of the dye molecules apparently diffuse during the adsorption process, which occurs by ion exchange with protons (DREXHAGE [1966]), into the underlying fatty-acid layers, to an extent which depends particularly on the composition of the adsorbing layer system (barium stearate, barium arachidate or cadmium arachidate), as was determined by energy-transfer experiments (DREXHAGE

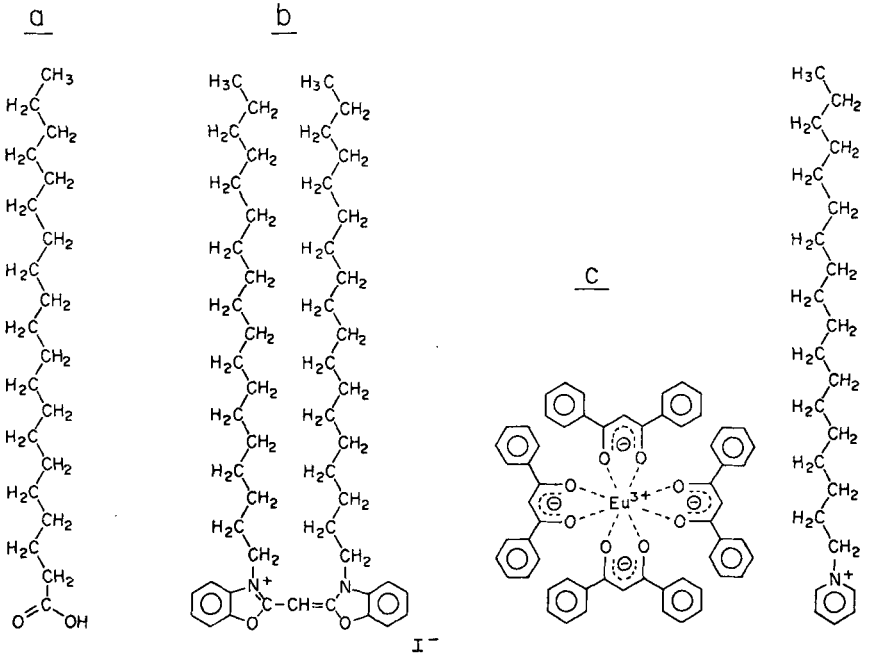

Fig. 4. Molecular structures of arachidic acid (a), *N,N'*-distearyloxacyanine iodide (b), and a europium dibenzoylmethane complex (c).

[1966], BARTH, BECK, DREXHAGE, KUHN, MÖBIUS, MOLZAHN, RÖLLIG, SCHÄFER, SPERLING, ZWICK [1966]). The irregularities in these dye layers can extend over distances of more than 100 Å, which renders them unsuitable for experimental testing of energy-transfer theories.

Very regular monomolecular dye layers can be prepared by a technique analogous to the deposition of CdC_{20} monolayers (DREXHAGE [1966], DREXHAGE and KUHN [1966], BÜCHER, DREXHAGE, FLECK, KUHN, MÖBIUS, SCHÄFER, SONDERMANN, SPERLING, TILLMANN, WIEGAND [1967]). The special dyes developed for this purpose (SONDERMANN [1971]) carry one or more stearyl substituents (Fig. 4) and hence have material properties very similar to long-chain fatty acids: When spread on a water surface, they stick the hydrophilic chromophore into the water, while the hydrophobic stearyl chains tend to point upward. Because all the work discussed in the later sections has been conducted with dye layers of this type, some details of their preparation will be reviewed.

A compound representative of the class of cyanine dyes is the oxacyanine derivative the structure of which is given in Fig. 4. Mixed monolayers of this dye and cadmium arachidate (molar mixing ratio of dye and CdC_{20} 1 : 10 or smaller) are obtained by spreading a chloroform solution that contains the components in the desired ratio on the same subphase (5×10^{-4} molar $CdCl_2$ solution) as is used for the preparation of cadmium–arachidate layers. Such films have properties very similar to CdC_{20} films and can be deposited in exactly the same fashion. In one dipping process a hydrophobic surface is covered with two monomolecular layers, whose chromophores are in close contact. Because the chromophores of the two layers are located practically in the same plane, such a bilayer can be regarded for many purposes as a single monomolecular dye layer. Many other dyes of this type can also be used to form mixed layers with cadmium arachidate, thus providing a wide range of wavelengths in absorption and fluorescence.

The spectra of absorption and fluorescence are rather broad with most organic dyes (Fig. 5). The peak absorption of a monomolecular layer is of the order of a few percent and decreases with decreasing mixing ratio between dye and CdC_{20}. The chromophores in cyanine-dye layers are oriented parallel to the surface, and the transition moments for absorption and fluorescence have this same orientation (see § 4). An important factor in fluorescence studies is the quantum yield of fluorescence. It varies considerably, even in a class of closely related dyes, and is quite high (nearly 100 %) in some monomolecular dye layers considered in this article. For instance, the blue fluorescence of a deposited oxacyanine monolayer (dye : CdC_{20} = 1:10) is intense enough to be visible in a partly darkened room, when excited with an ultraviolet lamp.

Besides the cyanine dyes, an entirely different fluorescent compound has been used extensively: a europium complex whose structure is also depicted

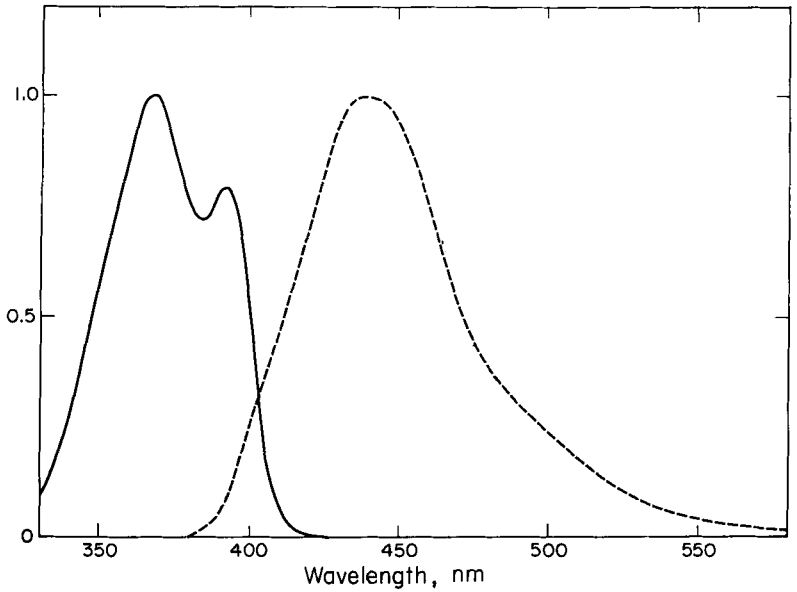

Fig. 5. Absorption (solid) and fluorescence (dashed) spectrum of mixed double layers of *N,N'*-distearyloxacyanine and cadmium arachidate (dye : CdC_{20} = 1 : 10); dye chromophores face to face.

in Fig. 4.* It has a strong absorption band with a maximum at 370 nm, which can be ascribed to the organic ligands. The energy absorbed in this band is rapidly transferred intramolecularly to the europium ion, which then fluoresces in a number of relatively narrow bands near 600 nm (see § 8). The decay time of the fluorescence is about 1 msec and therefore very convenient to measure. The transition moments of the fluorescence are randomly oriented, as would be expected from the highly symmetrical environment of the europium ion.

Monolayers of the pure europium complex are extremely viscous and for this reason cannot be deposited: The slide simply slips through the film without picking up a monolayer. However, on admixture of cholesterol in a molar ratio of 1 : 1 and under an increased surface pressure of 35 dyne/cm, smooth monolayer deposition on a hydrophobic surface is achieved (DREXHAGE [1966]). Monolayers showing particularly reproducible fluorescence were obtained on admixture of tripalmitin (molar ratio of dye and tripalmitin 1 : 3) under a surface pressure of 40 dyne/cm or of heptadecyl methyl ketone (molar ratio 1 : 2) under 30 dyne/cm. Since the viscosity of these films decreases with increasing temperature, it is sometimes useful to raise the water temperature by a few degrees above room temperature in order to ensure smooth deposition of the monolayer.

* The europium–dibenzoylmethane complex was prepared by Dr. W. Sperling, University of Marburg, with a procedure similar to the one of BAUER, BLANC, ROSS [1964].

The deposition of these monolayers requires much more attention than the preparation of CdC_{20} or mixed cyanine–dye layers. Because the europium complex is sensitive even to weak acids, its monolayers decompose slowly due to the influence of the free arachidic acid in the underlying and covering CdC_{20} layers, as can be judged from the gradual disappearance of the red fluorescence. Mixed layers with tripalmitin or heptadecyl methyl ketone are much more stable in this respect than the layers prepared with cholesterol. In contrast to the CdC_{20} and mixed cyanine-dye layers, the films of the europium complex are formed from a solvent mixture consisting of benzene and acetone in the volume ratio 4 : 1 on pure water without addition of a salt, whose p_H-value is maintained between 6.5 and 8.0 through the addition of a few drops of sodium–hydroxide solution. Even if prepared most carefully, the monolayer often is inhomogeneous in that some areas fluoresce more efficiently than others. Furthermore, fluorescence measurements on the deposited monolayers of this compound must be done under carefully controlled conditions, since, e.g., the fluorescence decay time depends on the temperature and on the oxygen content of the atmosphere surrounding the layer system.

From the method of preparation of these dye layers it is expected that the chromophores form a single layer of molecular cross-section. This hypothesis is supported by all optical experiments, in which the characteristic distance is about 1000 Å or larger. However, in experiments on energy transfer (critical distance about 100 Å) some differences between theory and experiment are observed (see § 7), which are most likely caused by irregularities in the dye–layer systems.

§ 3. Optical Properties of Cadmium–Arachidate Layers

In the work to be discussed in following sections, the monomolecular dye layers are embedded in a system of transparent cadmium–arachidate spacer layers. Knowledge of the thickness and the optical constants of this dielectric is the basis for the quantitative evaluation of the experiments.

3.1. DETERMINATION OF THE REFRACTIVE INDICES

It has been discovered by BLODGETT and LANGMUIR [1937] that multilayers of barium stearate are birefringent. They behave like positive uniaxial crystals with the optic axis oriented normal to the surface. This birefringence, which is obviously caused by the parallel alignment of the fatty-acid molecules within the film, is also observed with the cadmium–arachidate layers with which this article is primarily concerned.

To determine the ordinary refractive index n_o of a layer system,* the above authors coated glass plates of different refractive index with systems whose optical thickness was chosen to be a quarter wavelength. Whether

* Throughout this article the following notation is used: n_o for the ordinary and n_e for the extraordinary refractive index of a layer system; n_3 and n_1 for the refractive indices of the supporting glass and of air or an immersion liquid, respectively.

the intensity of the light, reflected by the sample, is decreased or increased by the $\lambda/4$-layer, depends upon the refractive indices of both the layer system and the substrate (BORN and WOLF [1970] p. 63). For normal incidence the reflectivity of one side of the sample is given by

$$R = [(n_1 n_3 - n_o^2)/(n_1 n_3 + n_o^2)]^2, \tag{3.1}$$

where n_1 and n_3 are the refractive indices of air and glass, respectively. Through the selection of glasses with appropriate refractive indices, the ordinary refractive index of the layers can be determined visually with a precision of three decimal places. With this method it was observed that $n_o = 1.491$ at $\lambda = 589$ nm for barium–stearate layers (BLODGETT and LANGMUIR [1937]). The ordinary refractive index of cadmium–arachidate layers, determined by the same technique, was found to be $n_o = 1.526$ for green light (DREXHAGE [1966]), whereas BLODGETT [1939] reported the value 1.54.

The accuracy of this technique can be slightly increased by a quantitative measurement of the reflectivity. In this case it would suffice to make measurements on only one sample, because the value of n_o can be calculated from R with the help of equation (3.1). However, the accuracy of the method is limited in any case by the ubiquitous thin layers of unknown refractive index on the glass surface, which influence the amplitude and phase of waves reflected at the layer–substrate boundary in an unpredictable way.

For the determination of the extraordinary refractive index n_e BLODGETT and LANGMUIR [1937] employed three different methods. In the first method a sequence of multilayer steps was deposited, in staircase fashion, on glass of high refractive index, and the reflectivity of the sample was examined in dependence on the angle of incidence. Due to interference between the waves, reflected at the air–layer and layer–glass boundaries, the reflectivity of the steps varies periodically with their optical thickness. The contrast between the different steps depends on the reflection coefficients at the boundaries involved and vanishes if one of these coefficients becomes zero. Thus, for light with the electric vector in the plane of incidence, the contrast disappears if the plate is viewed at Brewster's angle θ_{Br}.* Using the independently determined value of n_o, the extraordinary index n_e can then be calculated (see Appendix) with

$$\tan \theta_{Br} = (n_e/n_1)[(n_o^2 - n_1^2)/(n_e^2 - n_1^2)]^{\frac{1}{2}}. \tag{3.2}$$

The second method also employs a series of steps, deposited on high-index

* Throughout the article the angle of incidence on the side of the air or immersion liquid is denoted θ; inside the layer system the angle of incidence is called α for the wave normal and β for the ray (see Appendix).

glass or on chromium. Again the light reflected by the step sequence is investigated; however, now at a larger angle of incidence, where the contrast is high. The number $\bar{N}$ of monolayers that marks the difference in thickness between one step of minimum reflectivity and the next, is given by

$$\bar{N} n d_1 \cos \alpha = \tfrac{1}{2}\lambda. \tag{3.3}$$

Here d_1 is the thickness of a single layer, and α is the angle of incidence of the wave normal inside the layer system, which is related to the angle of incidence θ on the air side by Snell's law,

$$n \sin \alpha = n_1 \sin \theta. \tag{3.4}$$

The refractive index n of the layers depends, in the case of light polarized parallel to the plane of incidence, on the angle α (see Appendix):

$$n^{-2} = n_o^{-2} \cos^2 \alpha + n_e^{-2} \sin^2 \alpha. \tag{3.5}$$

Thus the value of n_e can be calculated from a measurement of $\bar{N}$ and θ and an independent determination of n_o and d_1.

The third method makes use of an optical compensator to determine the relative phase retardation of the ordinary and extraordinary rays. It is somewhat awkward, because a total of about 5000 deposited monolayers was needed for the measurement. Nevertheless, the results obtained by all three methods were in good agreement, and the value $n_e = 1.551$ ($\lambda = 589$ nm) was given by BLODGETT and LANGMUIR [1937] for barium-stearate layers.

Entirely different methods, which involve fluorescent dye layers, have also been used to determine the refractive indices n_o and n_e of CdC_{20} layers. The values $n_o = 1.522$ and $n_e = 1.59$ (both at $\lambda = 612$ nm) were observed by FLECK [1969] and $n_e = 1.60$ ($\lambda = 405$ nm) by FORSTER [1967]. Details of these measurements are given in § 8 and § 6, respectively. The remarkably strong birefringence ($n_e - n_o = 0.07$) of the CdC_{20} layers can not be ignored in quantitative experiments with monomolecular dye layers, as will become evident in the later sections.

3.2. DETERMINATION OF LAYER THICKNESS

All optical methods for the measurement of the layer thickness make use of multiple-beam interference in one way or another and involve a comparison of the thickness with the wavelength of the measuring light. We mention here only the three most important methods, which have yielded accurate values of the layer thickness.

The oldest technique (BLODGETT [1935]) employs plates of high-index glass, which are coated with a stair-like succession of fatty-acid layers. The

reflectivity of such a plate varies periodically with the optical thickness of the layer system, and the value of $\bar{N}$ is determined visually. The optical thickness $n_0 d_1$ of a single layer then follows from equation (3.3). In order to establish a sufficiently high contrast between the steps, the reflection coefficients at the air-layer and layer-substrate interface should be comparable, which is the case, if high-index glass is used as support for the layers. Instead of such glass a metal of low reflectivity, e.g., chromium or tantalum, can be used. In this case a particularly good contrast is obtained at large angles of incidence, where the reflection coefficient of the air–layer interface is relatively high (BLODGETT and LANGMUIR [1937]). Using the independently determined refractive index $n_0 = 1.491$, these authors found the value $d_1 = 24.40$ Å for the thickness of a barium–stearate monolayer.

Another now widely applied method, called ellipsometry, was introduced to the study of built-up layers by ROTHEN [1945]. Recently it was used in the case of CdC_{20} layers by ENGELSEN [1971] and STEIGER [1971]. In this method monochromatic light, plane polarized at 45° to the plane of incidence, is reflected from a metal surface at an oblique angle. Since the components in and perpendicular to the plane of incidence experience different changes in phase and amplitude, the reflected light is elliptically polarized. If a thin transparent layer is deposited on this metal surface, multiple-beam interference affects phase and amplitude of the two reflected components to a different degree, because the reflection coefficient of the layer–air interface is different for the two components. Obviously, the interference depends on the optical thickness of the applied layer, which is measured by the change in ellipticity of the reflected light. With a fairly simple apparatus the measurement can be made to an accuracy of ± 0.1 Å. The relation between the parameters of the ellipse and the layer thickness is rather complex, and it is practical to calibrate the apparatus with layers of known thickness and make relative measurements. In the case of birefringent layers the theory becomes even more complicated, because both the ordinary and the extraordinary ray are involved (ENGELSEN [1971]). Nevertheless, the technique has proven useful in many applications (ROTHEN [1968]). It has also been extended to transmission measurements (ENGELSEN [1972]).

A third method, conceptually very simple, is closely related to the work of Blodgett and Langmuir, the main difference being a quantitative measurement of the light intensities in place of visual observation (DREXHAGE [1966], DREXHAGE and KUHN [1966],* BÜCHER, DREXHAGE, FLECK, KUHN, MÖBIUS,

* In this paper Fig. 2b is incorrect. The correct plot is given by BÜCHER, DREXHAGE, FLECK, KUHN, MÖBIUS, SCHÄFER, SONDERMANN, SPERLING, TILLMANN, WIEGAND [1967] and in Fig. 7 of this article.

SCHÄFER, SONDERMANN, SPERLING, TILLMANN, WIEGAND [1967]). A microscope slide is coated on one side with an evaporated semitransparent silver mirror. A certain number N of the monolayers to be studied (total thickness $d = Nd_1$) is then deposited on top of the mirror, and the light transmission is measured, preferably with reference to another silver-coated slide of the

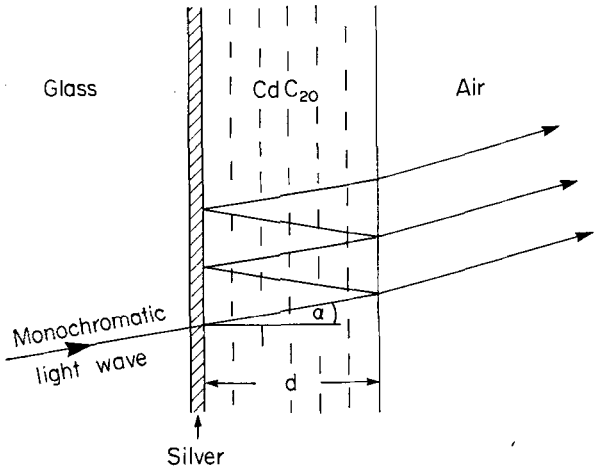

Fig. 6. Scheme for determining the thickness of fatty-acid layers. The transmission is modified by multiple interference within the layer system.

same initial transmission. The change in transmission that occurs due to multiple-beam interference within the layer is related to its optical thickness (Fig. 6), and the relative transmission T_s of the sample is given by the Airy function

$$T_s = G\tau^2 t_{21}^2/[1+\rho^2 r_{21}^2 - 2\rho r_{21}\cos(\phi-\delta)]; \tag{3.6}$$

$$\phi = 4\pi N n d_1 \cos\alpha/\lambda. \tag{3.7}$$

Here τ and t_{21} are the amplitude transmission coefficients for a light wave entering the layer system through the silver mirror and passing the layer–air interface, respectively. Similarly, ρ and r_{21} denote the amplitude reflection coefficients at the layer–silver and layer–air interface, whereas δ is the phase shift occurring on reflection at the layer–silver interface. The factor G takes into account the presence of the uncoated surface of the slide and the transmission T_r of the reference slide: $G = t_{13}^2/T_r(1-r_{31}^2 R_3)$. The quantity t_{13} is the transmission coefficient for light passing the air–glass interface, and r_{31} is the reflection coefficient for light incident from the glass onto this interface. Although the reflectivity R_3 of the system mirror + layers varies

with its thickness (see § 4), the value of G varies only slightly and may be considered constant in most practical cases.

According to equations (3.6) and (3.7) the relative transmission T_s is a periodic function of the number N of monolayers. Hence the thickness d_1 of a single cadmium–arachidate layer can be determined from a plot of T_s versus N (Fig. 7) if the refractive index n of the layers is known. With $n_0 = 1.526$ at $\lambda = 546$ nm and perpendicular incidence ($\cos \alpha = 1$) the value $d_1 = 26.4\ \text{Å} \pm 0.1\ \text{Å}$ was obtained from the data given in Fig. 7. Applying Fresnel's formulas one can calculate the quantities r_{21}, t_{21}, r_{31} and t_{13},

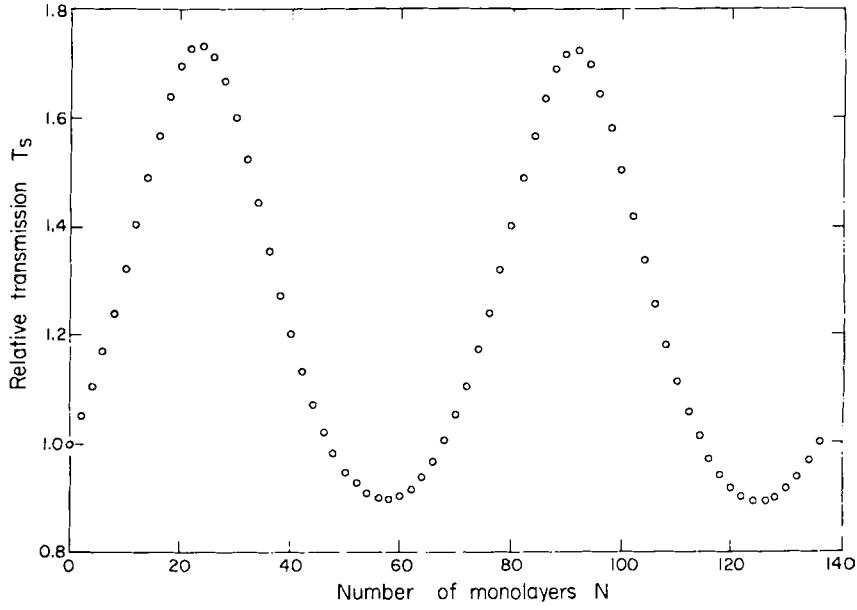

Fig. 7. Plot of relative transmission T_s versus number N of cadmium-arachidate layers prepared according to section 2.1. $\lambda = 546$ nm; $\alpha = 0$; $T_r = 0.240$. All values were obtained on the same sample by increasing N in steps of two at a time. (From DREXHAGE [1966].)

whereas ρ, τ and δ are dependent on the density of the silver coating and can be determined from the plot in Fig. 7. Values of T_s, calculated from equation (3.6) with the parameters so determined, agreed with those observed experimentally within $\pm 0.5\ \%$, indicating a very good reproducibility in the deposition of the CdC_{20} layers. It must be borne in mind, however, that all optical methods described here yield a layer thickness averaged over the irradiated area. Thus any microscopic irregularities, randomly incor-

porated into the layer system, would be averaged out and can not be detected with these methods.

The sensitivity of this method depends on the value of the product ρr_{21} (equation (3.6)). With a silver mirror of high reflection coefficient ($\rho > 0.8$) the relative transmission $T_s(N)$ can vary by more than the factor 2 (Fig. 7). Hence fairly accurate measurements can be accomplished even with commercially available photometers. It is particularly easy to make relative thickness determinations if monolayers of known thickness, e.g., CdC_{20} layers, are used for a calibration. The change in transmission that occurs on deposition of the layers of unknown thickness is compared with that produced by a certain number of CdC_{20} layers assuming the same refractive index for both. Furthermore the above technique can be used to determine the extraordinary refractive index n_e of layer systems, if the angle of incidence at which the relative transmission T_s becomes independent of N is measured (Brewster's angle, $r_{21} = 0$). With the otherwise determined ordinary index n_o the extraordinary index n_e is then obtained from equation (3.2).

It is to be mentioned here that there is a long-standing discrepancy between the thickness of monolayers measured by optical and by X-ray techniques, which has not yet been explained satisfactorily. The X-ray measurements yielded a markedly larger value of the thickness of barium–stearate layers than did the optical techniques described above (HOLLEY [1938], BERNSTEIN [1940]). A similar discrepancy in the case of CdC_{20} layers can be inferred from X-ray data reported by MANN, KUHN, SZENTPÁLY [1971], who found $d_1 = 28.0$ Å (at 20 °C).* Moreover, these authors report a temperature dependence of the X-ray determined thickness ($d_1 = 28.7$ Å at -35 °C), which has not been noticed by other workers. The optical value for CdC_{20} layers has been confirmed recently by BÜCHER [1970], who measured $d_1 = 26.5$ Å with a variation of the transmission method described above.

§ 4. Coherent Scattering at a Dye Monolayer

According to elementary dispersion theory a dye molecule can be considered as a damped electron oscillator, which carries out forced vibrations under the influence of the alternating electric field of a light wave. The oscillating electron is the source of a secondary wavelet which is coherent with the exciting light. In the case of many such molecules, i.e. bulk matter,

* Contrary to these findings an X-ray determined value $d_1 = 26.8$ Å is mentioned by STEIGER [1971].

all the secondary wavelets interfere with each other and with the exciting wave, thus giving rise to the known phenomena of absorption, reflection, refraction and dispersion. In fact, all optical properties of matter can be explained on the basis of such atomistic considerations (BORN and WOLF [1970] p. 84). Because of the huge number of molecules in a three-dimensional medium the treatment of the interference of primary and secondary waves is rather complicated. The often considered *plane layer of atomic oscillators* is realized experimentally by a monomolecular dye layer (DREXHAGE [1966]).

4.1. THE PHASE OF THE SCATTERED WAVE

When a plane wave of light impinges normally on a monomolecular layer of dye molecules the oscillators are excited into forced vibrations that occur in all molecules with the same phase. The phase is, however, dependent on the frequency ν of the exciting light and on the eigenfrequency ν_0 of the oscillators. In the case $\nu \ll \nu_0$ the oscillators vibrate in phase with the exciting wave, for $\nu = \nu_0$ with a phase lag of $\frac{1}{2}\pi$ and in the case $\nu \gg \nu_0$ in opposite phase. All the secondary wavelets emitted by the vibrating electrons are in phase and combine to form two plane waves propagating with and against the direction of the exciting wave (Fig. 8). It can be shown that the

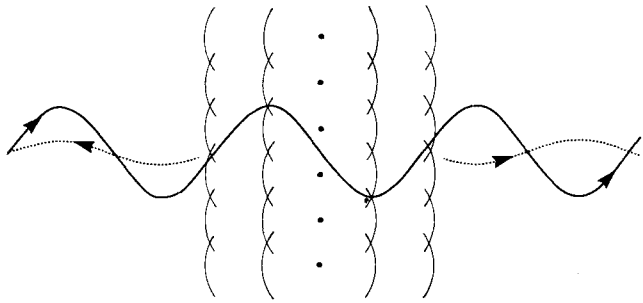

Fig. 8. Scattering at a layer of oscillators excited by a plane wave (solid). The spherical wavelets arising from the oscillators add up to plane waves (dashed) moving in backward and forward direction. In the case shown ($\nu = \nu_0$) the phase shift δ has the value π, and maximum attenuation of the exciting wave results.

phase of these scattered plane waves lags behind the phase of the oscillators by $\frac{1}{2}\pi$ (KUHN [1933] p. 340, KAUZMANN [1957] p. 600). The scattered plane waves have therefore a phase shift* of $\frac{3}{2}\pi$ for $\nu \ll \nu_0$, π for $\nu = \nu_0$ and $\frac{1}{2}\pi$ for $\nu \gg \nu_0$ with respect to the incident wave. This phase shift is directly related to the phase of the oscillators themselves.

* As usual the term phase shift denotes a *forward* shift of the phase.

The forward-scattered wave interferes with the exciting wave, which thus is attenuated in the region of resonance (Fig. 8), but merely shifted in phase at frequencies that are remote from the eigenfrequency. The backward-scattered, i.e. reflected, wave is of extremely small intensity (about 10^{-4} times the incident intensity in the region of resonance). However, its amplitude is only about ten times smaller than the amplitude of a wave reflected at the layer–air interface, which makes simple interference experiments feasible.

In order to determine the phase shift of the reflected wave, a glass plate is coated with a monomolecular dye layer,* which then is covered with a number of (non-absorbing) CdC_{20} layers (DREXHAGE [1966]). The transmission of such a layer system (Fig. 6 with dye layer in place of the silver film) is in analogy to equation (3.6) given by

$$T = (n_1/n)\tau^2 t_{21}^2/[1+\rho^2 r_{21}^2 - 2\rho r_{21}\cos(\phi-\delta)]. \tag{4.1}$$

It is assumed here, that the refractive indices of glass and CdC_{20} layers are identical. The quantities τ and ρ are here the amplitude transmission and reflection coefficients of the dye layer, whereas δ is the phase shift of the wave reflected at the dye layer. If both sides of the slide are coated with

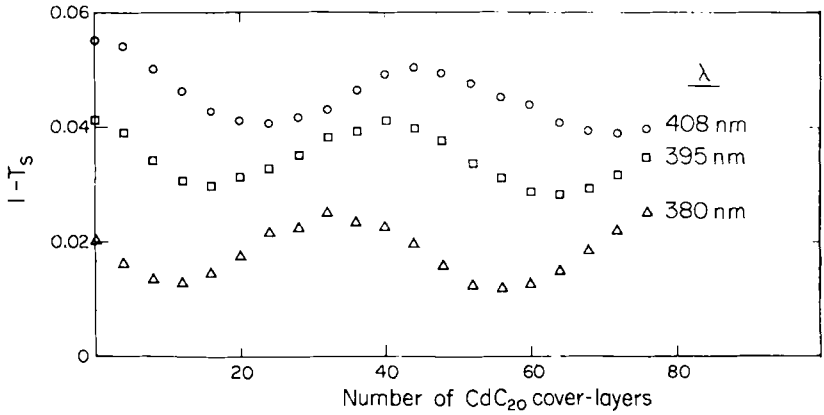

Fig. 9. Relative transmission T_s of a glass plate coated with a dye double layer on both sides as function of the number of CdC_{20} cover-layers for three different wavelengths within the absorption region of the dye (normal incidence). Values obtained on the same sample by increasing N in steps of four at a time. Dye double layers (chromophores face to face) consist of *N,N'*-distearylthiacyanine and cadmium arachidate (dye : CdC_{20} = 1 : 10). (From DREXHAGE [1966].)

* Here and elsewhere it is understood that the glass plate is coated with, say, five CdC_{20} layers, before the dye monolayers are deposited. Dye monolayers, deposited on the hydrophilic glass surface, often show erratic optical properties.

identical layer systems, the transmission T_s of the sample relative to an uncoated slide (transmission T_r) is described by

$$T_s = T^2/[T_r(1-R_3^2)]. \tag{4.2}$$

The quantity R_3 denotes the reflectivity of the layer system for light incident from the glass. In all practical cases R_3^2 is so small that it can be neglected in equation (4.2).

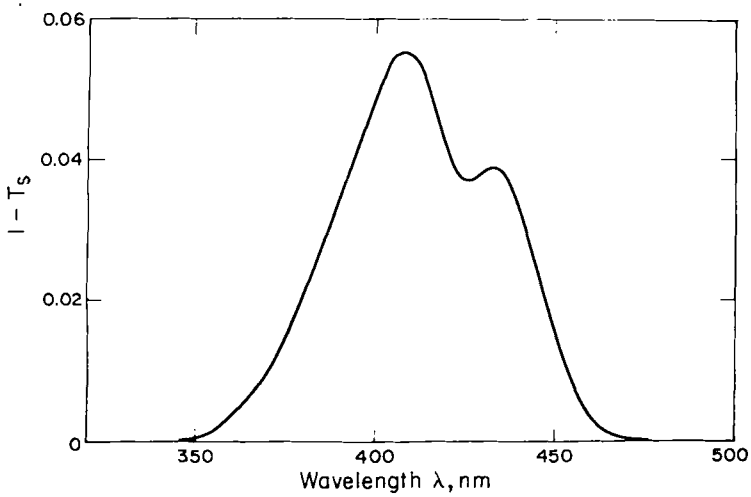

Fig. 10. Relative transmission T_s of the sample of Fig. 9 without additional CdC_{20} coverlayers as function of the wavelength λ (normal incidence). (From DREXHAGE [1966].)

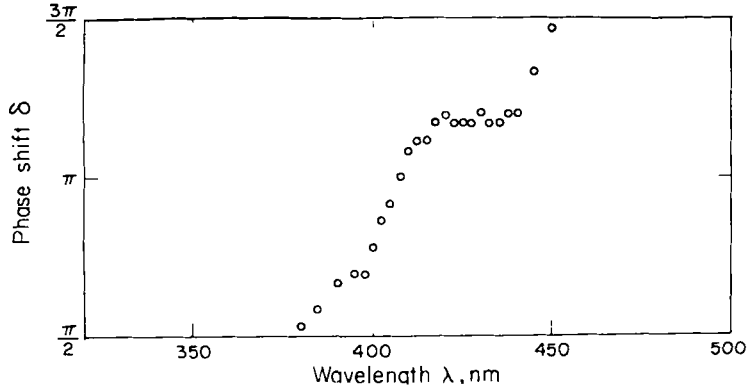

Fig. 11. Phase shift δ of the light wave reflected at a monomolecular dye layer as function of the wavelength λ; same sample as in Figs. 9 and 10. (From DREXHAGE [1966].)

According to equations (4.1), (3.7) and (4.2), the transmission T_s is expected to be a periodic function of the number of CdC_{20} cover-layers. Experimentally this was indeed observed for a number of different wavelengths (Fig. 9). It is obvious from this figure that the phase shift δ varies with the wavelength of the exciting light, and the plot of δ as a function of the wavelength λ (Fig. 11) exhibits the expected variation throughout the absorption band of the dye (Fig. 10). The shoulder in the plot of δ versus λ reflects a shoulder in the absorption spectrum.

From such data as shown in Fig. 9 the reflection coefficient ρ of the dye monolayer can also be determined. At the wavelength at which $\delta = \pi$ (Fig. 8) ρ is expected to be $1-\tau$. A reasonably good agreement was observed in both cases studied (DREXHAGE [1966], ELSNER [1969]).

4.2. THE REFLECTIVITY OF DYE LAYER SYSTEMS

The wave, scattered backward by a dye monolayer, affects not only the transmission, but also the reflectivity of a monolayer system. In fact, the influence upon the reflectivity is the more pronounced, as was shown by DREXHAGE [1966] and BÜCHER [1970]. The basic features of the effect become clear from an inspection of Fig. 12. Depending on the phase shift δ and on the distance d, the interference between the wave, reflected at the dye layer, and the wave, reflected at the layer–air interface, may be constructive or destructive. Accordingly, the reflectivity of the layer–air interface is enhanced or reduced by the incorporated dye layer.

In order to calculate the reflectivity of such a thin film all partial waves are added in the usual manner (MAYER [1950] p. 144, WOLTER [1956]), and for the reflectivity R_1 (light incident from the air) and R_3 (light incident from the glass) the following expressions are obtained (DREXHAGE [1966]):

$$R_1 = [\rho^2 + r_{21}^2 - 2\rho r_{21} \cos(\phi - \delta)]/[1 + \rho^2 r_{21}^2 - 2\rho r_{21} \cos(\phi - \delta)], \tag{4.3}$$

$$R_3 = \frac{\rho^2 + r_{21}^2(\tau^4 + \rho^4 - 2\tau^2\rho^2 \cos 2\delta) + 2\tau^2 \rho r_{21} \cos(\phi + \delta) - 2\rho^3 r_{21} \cos(\phi - \delta)}{1 + \rho^2 r_{21}^2 - 2\rho r_{21} \cos(\phi - \delta)} \tag{4.4}$$

Since the uncoated side of the plate gives rise to multiple reflections, the reflectivities R_{s1} and R_{s3} of the sample with reference to an uncoated glass plate (reflectivity R_r) are given by

$$R_{s1} = [R_1 + r_{21}^2(T^2 - R_1 R_3)]/[R_r(1 - r_{21}^2 R_3)] \tag{4.5}$$

and

$$R_{s3} = [r_{21}^2 + R_3(1 - 2r_{21}^2)]/[R_r(1 - r_{21}^2 R_3)]. \tag{4.6}$$

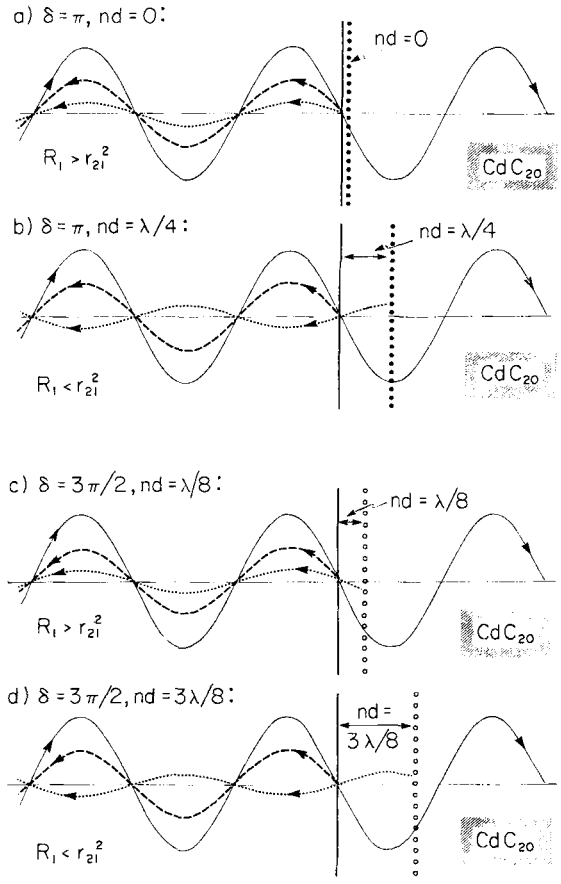

Fig. 12. Influence of a monomolecular dye layer on the reflectivity of the interphase between air and CdC_{20} layers (light incident from the air). Cases a) and b): wavelength of light corresponding to absorption maximum of dye, $\delta = \pi$; cases c) and d): wavelength of light much greater, $\delta = \frac{3}{2}\pi$. Reflectivity is enhanced (cases a) and c)) or decreased (cases b) and d)) depending on the optical path *nd*. Amplitudes of reflected waves are not to scale.

Here it is again assumed that the refractive indices of glass and CdC_{20} layers are identical. The experimentally observed reflection spectra $R_{s1}(\lambda)$ and $R_{s3}(\lambda)$ (Fig. 13) were found in good agreement with equations (4.5) and (4.6), if $\tau(\lambda)$ was taken from the absorption spectrum.

It is noteworthy that the dye monolayer has an influence on the reflectivity even at wavelengths where it does not show any absorption ($\frac{1}{8}\lambda$-curves in Fig. 13). This reflects the fact that the electron oscillators still vibrate with a significant amplitude even at these frequencies remote from resonance.

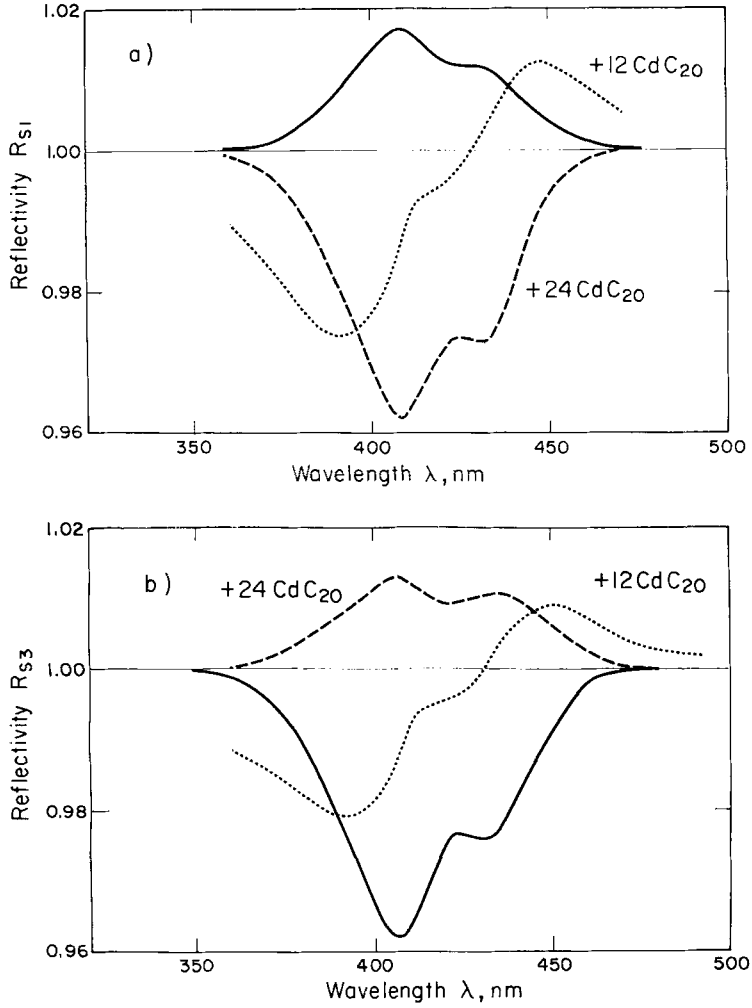

Fig. 13. Reflectivity of a glass plate carrying on one side a single dye layer (*N,N'*-distearylthiacyanine : $CdC_{20} = 1 : 10$) relative to an uncoated glass plate; light incident a) from the air and b) from the glass. Solid curve: no additional CdC_{20} layers. The addition of 12 or 24 CdC_{20} layers corresponds to an optical path of $\sim\frac{1}{8}\lambda$ and $\sim\frac{1}{4}\lambda$, respectively. (From BÜCHER [1970].)

However, since the phase shift δ is $\frac{1}{2}\pi$ or $\frac{3}{2}\pi$, no attenuation of the incident wave occurs. In the case of a three-dimensional medium this corresponds to the familiar situation that, while there is no light absorption, the wavelength in the material is different from vacuum (refractive index greater or smaller than unity).

More complicated interference systems, involving a dye monolayer, have been treated by BÜCHER [1970]. He showed theoretically as well as experimentally that the transmission of an interference filter, which contains a monomolecular dye layer between two metal mirrors, can only be understood, if the reflection at the dye layer is taken into account. This is essential for a correct interpretation of studies on electrochromism, in which the absorption of the dye layer is changed under the influence of an electric field (BÜCHER [1970], BÜCHER and KUHN [1970]*). Because in several related papers (BÜCHER, WIEGAND, SNAVELY, BECK, KUHN [1969], SCHMIDT, REICH, WITT [1969, 1971], KLEUSER and BÜCHER [1969], SCHMIDT and REICH [1972a, b]) this difficulty was not appreciated, the interpretation of the experimental results given there is in doubt.

The absorption and reflection spectra of monomolecular dye layers have been measured with sensitive single-beam photometers, which were described by DREXHAGE [1964], BÜCHER, ELSNER, MÖBIUS, TILLMANN, WIEGAND [1969] and BÜCHER [1970].

4.3. THE ABSORPTION OF DYE LAYER SYSTEMS

We have seen that the light response of a monomolecular dye layer, embedded in a system of CdC_{20} layers, can be understood by describing the dye molecules as elementary oscillators, which coherently emit secondary waves of the same frequency as the exciting light. This must not be confused with the emission of fluorescence, which takes place after the absorption of energy by the oscillators and which is not coherent with the exciting radiation and generally of lower frequency. Some details of fluorescence emission will be covered in later sections.

It was shown that the transmission T and the reflectivities R_1 and R_3 of a dye layer system can be calculated by considering the waves scattered by the dye layer. The absorption, i.e. the fraction of the incident light energy, absorbed in the dye layer, can then be found from the identities

$$A_1 + R_1 + T = 1; \qquad A_3 + R_3 + T = 1. \tag{4.7}$$

The value of T is independent of the direction of irradiation. However, in unsymmetrical layer structures like the one shown in Fig. 6, the reflectivity is generally dependent on the direction of incidence, as is evident from equations (4.3) and (4.4). Therefore the amount of light energy absorbed by the

* The expression for the transmission of a dye layer between metal films, used in this paper, is incorrect, since it is based on the presumption that absorption and transmission are complimentary. However, the error thus made is only about 15 % because of the low reflectivity of the metal films and is smaller than the experimental errors.

dye layer depends on the direction of irradiation, and we must distinguish between the quantities A_1 (light incident from the air) and A_3 (light incident from the glass), which can be calculated from equations (4.1), (4.3), (4.4) and (4.7). If the absorption is very weak, as is usually the case with monomolecular dye layers, it is obtained for normal incidence (DREXHAGE [1966])

$$A_1 \approx A(1-r_{21}^2); \tag{4.8}$$

$$A_3 \approx A[1+r_{21}^2+2r_{21}\cos(4\pi n_0 d/\lambda)]. \tag{4.9}$$

Here A denotes the absorption of the dye layer embedded in an extended isotropic medium, i.e. $n_1 = n_0 = n_3$.

The relations (4.8) and (4.9) can be immediately understood, if it is realized that for small absorptions the absorbed energy is proportional to the square of the local field amplitude. When the light is incident from the side of the glass, a standing light wave (see § 5) is formed in front of the layer–air boundary, whose amplitude E_d is given by $E_d = E_0\,[1+r_{21}^2+2r_{21}\cos(4\pi n_0 d/\lambda)]^{\frac{1}{2}}$. In the other case (light incident from the air) the dye layer is not within a region of standing light waves, and thus the absorption A_1 is independent of the distance d. The marked variation of A_3 with distance d (by a factor of 2.3 in the systems considered here!) can not be ignored in quantitative monolayer studies. In order to circumvent the distance dependence of the absorption, it is sometimes advisable to irradiate dye layer systems from the side of the air.

The quantity A can be obtained from measurements of the transmission T as a function of $d = Nd_1$ (Fig. 9). For small values of A (e.g., $A \leqq 0.1$), it is only necessary to determine the maximum and minimum values of the function $T(d)$ (DREXHAGE [1966]):

$$A = 1-\tfrac{1}{2}(T_{\max}+T_{\min}). \tag{4.10}$$

It is important to note that the quantities A, A_1 and A_3 are, in general, different from each other and from $1-T$. In particular, $1-T$ is not to be confused with one of the absorptions, as is done quite often in the published literature, including earlier papers by this author. If both sides of the glass are coated with identical layer systems, the absorption A of one dye layer can be obtained in analogy to equation (4.10) from

$$A = \tfrac{1}{2}-\tfrac{1}{4}(T_{s,\max}+T_{s,\min}). \tag{4.11}$$

4.4. THE ORIENTATION OF THE DYE CHROMOPHORES

Because the chromophores of most organic dyes are anisotropic, it is to be expected that a non-random orientation of the dye molecules in the

monolayer gives rise to dichroism, i.e. a dependence of the absorption on the polarization of the light. In fact, this phenomenon has been used to determine the orientation of the chromophores (DREXHAGE [1966], TILLMANN [1966], BÜCHER, DREXHAGE, FLECK, KUHN, MÖBIUS, SCHÄFER, SONDERMANN, SPERLING, TILLMANN, WIEGAND [1967]). The slide coated with the dye layer was irradiated at an angle $\theta \neq 0$, and the transmission was measured with light, polarized perpendicular and parallel to the plane of incidence.

Due to the refraction at the air–layer boundary the light traverses the dye layer at the angle α (equation (3.4)), and for perpendicular polarization the absorption $A_\perp$ is given by

$$A_\perp = A/\cos\alpha = An_o/(n_o^2 - \sin^2\theta)^{\frac{1}{2}}. \tag{4.12}$$

The increase of the absorption by the factor $1/\cos\alpha$ is caused by the increased number of dye molecules seen by the light and occurs for both polarizations.* In the case of parallel polarization, however, the absorption $A_\parallel$ depends in addition on the particular orientation of the chromophores. We may distinguish the following cases:

a) transition moments randomly oriented,

$$A_\parallel = A/\cos\alpha = An_o/(n_o^2 - \sin^2\theta)^{\frac{1}{2}}; \tag{4.13}$$

b) transition moments randomly oriented in layer plane,

$$A_\parallel = A\cos\alpha = A(n_o^2 - \sin^2\theta)^{\frac{1}{2}}/n_o; \tag{4.14}$$

c) transition moments perpendicular to layer plane,

$$A_\parallel = A'\sin\alpha\tan\alpha = A'\sin^2\theta/[n_o(n_o^2 - \sin^2\theta)^{\frac{1}{2}}]. \tag{4.15}$$

Since $A = 0$ in case c, the symbol A' is used here for the absorption. For the dichroic ratio $D = A_\perp/A_\parallel$ we obtain from the above relations in case a $D = 1$, in case b $D = n_0^2/(n_0^2 - \sin^2\theta)$ and in case c $D = 0$. At the (often used) angle of incidence $\theta = 45°$ and with $n_o = 1.53$ we obtain from equations (4.12) to (4.15) $A_\perp = 1.13\,A$ and in

case a: $A_\parallel = 1.13\,A$, $D = 1$;
case b: $A_\parallel = 0.89\,A$, $D = 1.27$;
case c: $A_\parallel = 0.24\,A'$, $D = 0$.

For the practical determination of $A_\perp$ and $A_\parallel$ one has to proceed, as was described in section 4.3 for the quantity A, i.e. one measures the transmission of the sample as function of the distance d and calculates $A_\perp$ and $A_\parallel$ in

* For the sake of simplicity we neglect here the birefringence of the layers and assume $n = n_o$ for both polarizations.

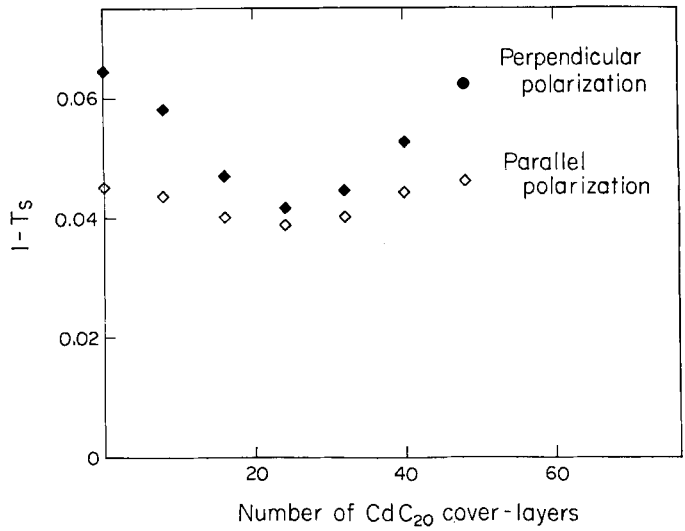

Fig. 14. Relative transmission T_s of a glass plate coated with a dye double layer on both sides as function of the number of CdC_{20} cover-layers for $\lambda = 408$ nm and oblique incidence ($\theta = 45°$). Same dye layers as in Figs. 9, 10 and 11. (From DREXHAGE [1966].)

analogy to equation (4.10) or (4.11). In case of the cyanine–dye monolayers (Fig. 14) considered in sections 4.1 and 4.2, it was observed experimentally at the wavelength of maximum absorption ($\lambda = 408$ nm): $A_\perp = 1.13\,A$ and $D = 1.26$ (DREXHAGE [1966]). From the latter value it could be concluded that the transition moments are oriented according to case b. It is to be noted that a qualitative observation of a dichroism in *transmission* measurements does *not* allow the above conclusion to be drawn, as was erroneously stated, e.g., in the article by BÜCHER, DREXHAGE, FLECK, KUHN, MÖBIUS, SCHÄFER, SONDERMANN, SPERLING, TILLMANN, WIEGAND [1967]. Even in case of random orientation of the transition moments (case a, $A_\perp = A_\parallel$) the transmission is different for the two polarizations.

The agreement between the experimentally determined values of $A_\perp$ and $A_\parallel$ and the theory given above is of particular interest, as it shows that the laws governing reflection and refraction at a dielectric boundary apply even at a distance as small as about 25 Å.

§ 5. Standing Light Waves

When two waves of the same frequency, travelling in opposite directions, interfere with each other, a so-called standing wave is formed. In the case

of light waves this phenomenon was first demonstrated by WIENER [1890] with a thin layer of photographic emulsion, and somewhat later by DRUDE and NERNST [1892] with a fluorescent film. By using a monomolecular dye layer as a probe standing light waves can be studied with greatly enhanced resolution (DREXHAGE [1966], DREXHAGE and KUHN [1966], BÜCHER, DREXHAGE, FLECK, KUHN, MÖBIUS, SCHÄFER, SONDERMANN, SPERLING, TILLMANN, WIEGAND [1967], DREXHAGE [1970b]).

In these experiments a microscope slide was coated with a highly reflecting silver or gold mirror and then covered with a stairlike succession of CdC_{20} layers. This was done by making successive dips, each of which was a few millimeters shorter than the previous one. On top of these CdC_{20} stairs a monomolecular layer of a fluorescent dye was deposited. Thus the dye molecules are separated from the mirror by a stepwise increasing distance, which is determined by the number of underlying CdC_{20} layers.

If the slide is irradiated with monochromatic light polarized perpendicular to the plane of incidence, the incident and reflected wave interfere, and the resultant electric-field amplitude E_d is given by

$$E_d = E_0[1+\rho^2+2\rho\cos(4\pi n_0 d\cos\alpha/\lambda-\delta)]^{\frac{1}{2}}. \tag{5.1}$$

Here we neglect the reflection at the air–layer boundary and assume nearly perpendicular incidence on the mirror, whose amplitude reflection coefficient and phase shift are called ρ and δ, respectively. At large angles of incidence and with polarization perpendicular to the plane of incidence, the reflection at the air–layer boundary can not be ignored; on the other hand, with parallel polarization the standing-wave phenomenon is more complicated owing to the fact that the electric vectors of incident and reflected wave have different directions (WOOD [1934] p. 210, BORN and WOLF [1970] p. 277).

For weak absorptions the energy absorbed by the dye layer is proportional to the square of the local electric-field amplitude E_d. The fluorescence intensity is proportional to the absorbed energy and is expected to be extremely small at the nodes of the standing wave, which occur at distances d_i, given by the condition

$$4\pi n_0 d_i\cos\alpha/\lambda-\delta = (2i-1)\pi;\quad i = 1, 2, 3\ldots. \tag{5.2}$$

Between these nodes the absorption and thus the fluorescence intensity should vary according to equation (5.1) and reach maxima at distances d_j (antinodes), given by

$$4\pi n_0 d_j\cos\alpha/\lambda-\delta = 2(j-1)\pi;\quad j = 1, 2, 3\ldots. \tag{5.3}$$

It was found that the experimentally observed position of the nodes agreed

very well with equation (5.2) (DREXHAGE [1966]). However, the fluorescence intensity on the steps between the nodes does *not* follow equation (5.1), and, moreover, the fluorescence color depends on the distance from the mirror (Fig. 15). This phenomenon is caused by an influence of the mirror on the fluorescence which will be discussed in § 8. This side effect makes it very difficult to verify equation (5.1) quantitatively in the particular case described. It should be possible to eliminate this difficulty, if instead of a metal mirror a dielectric reflector were used that has a high reflectivity for the wavelength of the exciting light, but low reflectivity for the wavelengths of the fluorescence.

The position of the nodes of the standing wave depends on the phase shift δ (equation (5.2)), which is dependent on the mirror material. This can be demonstrated with a slide coated with adjacent films of silver and gold, before the whole is covered with an identical layer system. The relative displacement of the standing-wave patterns in front of the silver and gold mirror, as seen in Fig. 15b, is a direct manifestation of the difference in phase shifts between the two metals. Furthermore, it can be seen from Fig. 15b, that the fluorescence intensity at the antinodes is smaller in front of the gold mirror than in front of the silver mirror. This is readily explained in terms of the reflection coefficient ρ, which is smaller for gold than for silver (equation (5.1)).

As was mentioned in section 4.3, the standing wave in front of a layer–air boundary can have a marked influence on the amount of light absorbed by a dye monolayer. This can be shown with a slide that is coated on one side with a monolayer of a fluorescent dye and then covered with a stair-like succession of CdC_{20} layers (DREXHAGE [1966]). If the exciting light is incident from the side of the air (Fig. 16, top), the dye layer is not within the region of a standing wave, and therefore the fluorescence intensity appears uniform (no dependence on the distance d). If, on the other hand, the layer

Fig. 15. Standing light waves in front of metal mirror, probed by a monomolecular layer of a fluorescent dye. Wavelength of illumination 366 nm, angle of incidence $\theta = 30°$, spacing d increasing from left to right in steps of 6 CdC_{20} layers (a) and of 4 such layers (b), silver mirror (a and b, upper half) and gold mirror (b, lower half). Mixed dye layers (double layers, chromophores face to face) consist of *N,N'*-distearyloxacyanine, *N,N'*-distearyloxacarbocyanine and tripalmitin (a), and of *N,N'*-distearyloxacyanine, *N,N'*-distearylthiacyanine and cadmium arachidate in the ratio 1 : 1 : 20 (b); ultraviolet exciting light absorbed by the oxacyanine, fluorescence in the green and yellow emitted by the second dye following energy transfer. Plate a viewed at two different angles. High speed Ektachrome. – No fluorescence on steps with dye at a node of standing wave, moderate to strong fluorescence at antinodes. Intensity and color of fluorescence depend on spacing d and on viewing angle (§ 8). Differences in phase shift and reflectivity between silver and gold mirror become apparent in plate b.

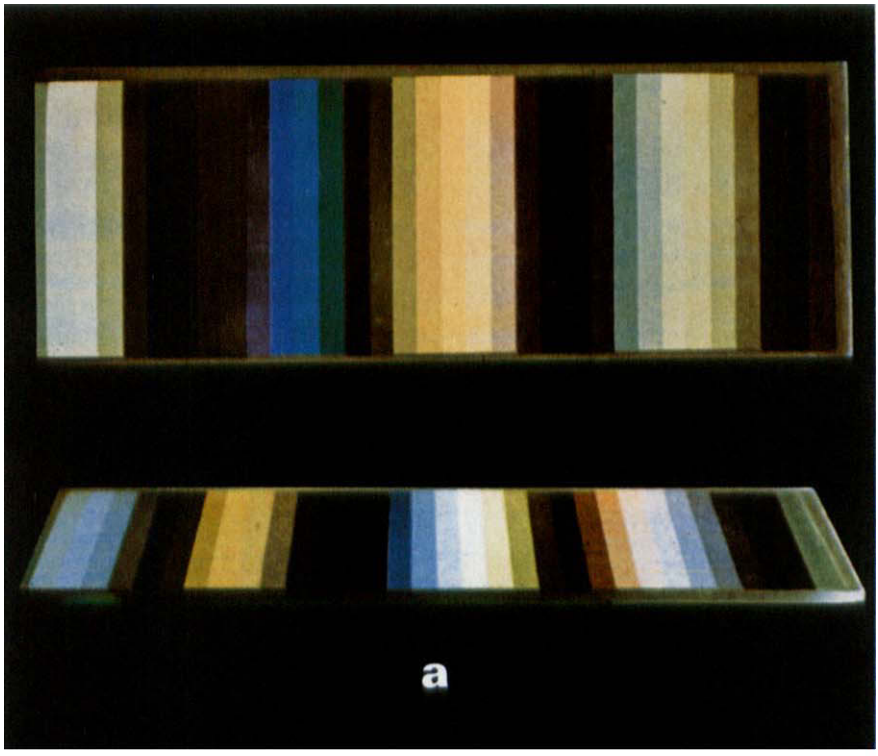
a

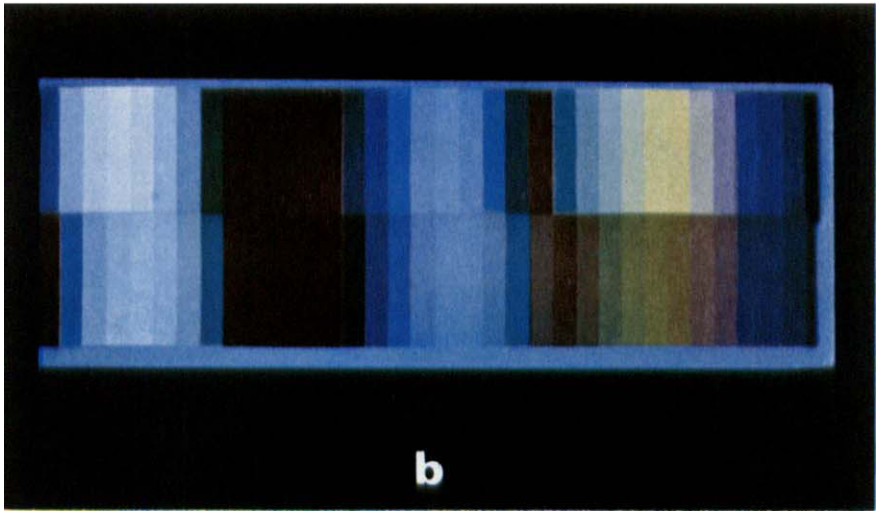
b

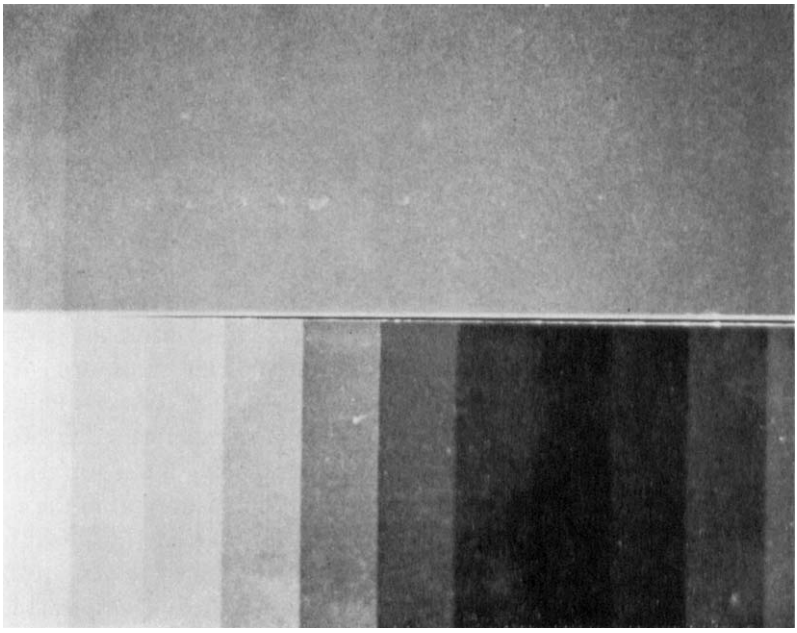

Fig. 16. Standing light waves in front of layer–air boundary, probed by a fluorescent dye layer. Identical glass plates coated on one side with a monomolecular dye layer and covered with a stair-like succession of CdC_{20} layers; spacing d increasing from left to right in steps of 4 such layers; same dye layers as in Fig. 15b, wavelength of illumination 366 nm, angle of incidence $\theta = 30°$. Top: irradiation of the layer system from the air, dye *not* within region of standing waves; bottom: irradiation from the glass side, absorption and fluorescence intensity vary with distance from boundary.

system is irradiated from the glass side (Fig. 16, bottom), the dye layer probes the standing wave in front of the layer–air interface, and thus the absorption varies with the distance d according to equation (4.9). The fluorescence intensity in this case appears at small distances (steps at the very left) much stronger than in Fig. 16, top, at any distance. While the effect is partly due to the described variation in the absorption, it is further enhanced by the influence of the reflecting boundary on the fluorescence emission (§ 8).

The absorption of all the dyes that have been used in monolayer studies so far, is due to electric-dipole transitions. Therefore their absorption is proportional to the square of the local electric-field amplitude and, in case of a standing light wave, shows minima at the distances d_i that are given by equation (5.2). However, at these same distances the magnetic-field amplitude has maxima, which would give rise to maximum absorption, if a dye were used, whose absorption is due to a magnetic-dipole transition. Similarly,

a dye with an electric-quadrupole transition would probe the electric-field gradient in front of the mirror and would show a pattern like the magnetic-dipole absorber.

§ 6. Evanescent Light Waves

When a light wave is incident on the boundary between two media of different refractive index at an angle greater than the critical angle, it is totally reflected. Nevertheless, one expects a wave in the second (less dense) medium, whose amplitude decays exponentially with increasing distance from the surface. It is, therefore, called a surface or evanescent wave. While this phenomenon has been studied quantitatively with microwaves long ago (SCHAEFER and GROSS [1910]), it is very difficult to examine in the case of light, because it is confined to a narrow region of only a few wavelengths in thickness. Compared with earlier qualitative demonstrations of the effect (WOOD [1934] p. 418), the monolayer technique has made feasible a very precise investigation of the properties of evanescent light waves. In these experiments a monomolecular layer of a fluorescent dye was placed by means of CdC_{20} layers at a well defined distance from the boundary, and the fluorescence excited by the evanescent wave was measured. Because the absorption of such a dye layer is very small (< 0.01), the inevitable disturbance of the phenomenon of total reflection is negligible. In a related experiment the emission of evanescent waves by fluorescent molecules has also been studied.

6.1. THE DECAY OF EVANESCENT WAVES

In order to examine the decay law of the evanescent wave a glass plate is coated on one side with a monomolecular layer of a fluorescent dye, which then is covered with a stepwise increasing number of CdC_{20} layers (FORSTER [1967], DREXHAGE and FORSTER [1967], DREXHAGE [1970b]). The plate is immersed in a liquid of a refractive index n_1, which is higher than n_o and n_e, and irradiated with a beam of monochromatic light at an angle θ greater than the critical angle of total reflection (Fig. 17). The evanescent wave occurring in the layer system is detected through the fluorescence emitted by the dye molecules. Because the distance d between the surface of the layer system and the dye molecules is established by the monomolecular CdC_{20} layers covering the dye layer, the decay of the evanescent wave is probed with high precision by measuring the relative fluorescence intensity on the various steps of the sample.

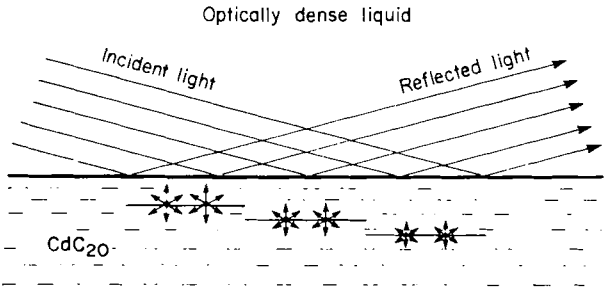

Fig. 17. Evanescent wave accompanying total reflection can be probed by monomolecular layers of fluorescent dyes. Intensity of fluorescence is proportional to the square of local field amplitude.

Theoretically the electric-field amplitude $E_\perp$ of the evanescent wave is given by (BORN and WOLF [1970] p. 47)

$$E_\perp \sim \exp\left[-(2\pi d/\lambda)(n_1^2 \sin^2\theta - n_o^2)^{\frac{1}{2}}\right]. \tag{6.1}$$

Here we confine ourselves to the case of polarization perpendicular to the plane of incidence. The energy absorbed by the dye molecules is proportional to $E_\perp^2$. The intensity of the fluorescence, emitted by the dye layer and measured according to Fig. 17, is affected by the layer-liquid boundary. As will be discussed in § 8, the fluorescence intensity I_d emitted at the angle α_{fl} with the normal to the boundary is given by (FORSTER [1967])

$$I_d = I_0[1 + r_{21}^2 + 2r_{21}\cos(4\pi n_o d \cos\alpha_{fl}/\lambda_{fl})], \tag{6.2}$$

where r_{21} is the Fresnel reflection coefficient of the layer–liquid boundary and λ_{fl} the wavelength of the fluorescence. Because the fluorescence was observed at an angle $\theta_{fl} = \frac{1}{2}\pi - \theta$, the refraction at the back of the slide must be taken into account by applying Snell's law ($n_o \sin\alpha_{fl} = n_1 \sin\theta_{fl}$). According to equation (6.2) the quantity I_0, which is proportional to $E_\perp^2$, is modified considerably (up to about 10 % in the described experiment) with variation of the distance d. It must be calculated from the measured fluorescence intensity I_d with equation (6.2). A logarithmic plot of I_0 as function of the distance d was found to agree very well with the exponential decay, expected from relation (6.1), for several angles of incidence θ (Fig. 18).

Because the CdC_{20} layers are attacked by organic solvents, an aqueous solution must be used as liquid of high refractive index. In the experiments discussed in this section a saturated solution of a 1 : 1 mixture of thallous formate and thallous malonate (Clerici's solution) in water was chosen, whose refractive index $n_1 \approx 1.7$, although somewhat de-

pendent on the temperature, is high enough to provide a large angular region of total reflection. However, this liquid usually shows some fluorescence of its own, which interferes with the fluorescence of the dye layer. In order to reduce this background fluorescence, dye layers containing a mixture of two cyanine dyes have been employed successfully (FORSTER [1967]). Here one dye serves as absorber for the exciting light ($\lambda = 405$ nm), and the second dye emits fluorescence ($\lambda_{fl} \approx 580$ nm), after an energy transfer between the dyes has taken place. The fluorescence of the dye layer is thus shifted toward wavelengths different from the fluorescence of the Clerici solution and can be isolated by means of filters.

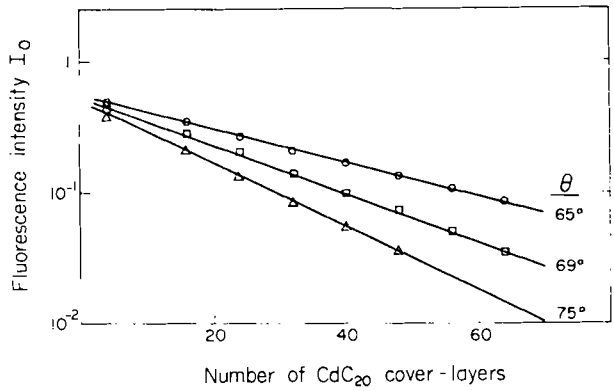

Fig. 18. Evanescent waves: logarithmic plot of fluorescence intensity I_0 as function of the number of CdC_{20} cover-layers for varying angles of incidence (perpendicular polarization). Experimental points obtained with eq. (6.2) from measured values I_d. $\lambda = 405$ nm, $n_0 = 1.526$, $n_1 = 1.728$; fluorescence maximum 580 nm. Mixed dye layers (double layers, chromophores face to face) consist of *N,N'*-distearylthiacyanine, *N,N'*-distearylindocarbocyanine and cadmium arachidate in the ratio 4 : 1 : 110. Lines represent theoretical decay calculated from eq. (6.1). (From DREXHAGE and FORSTER [1967].)

Whereas in the above experiments the angle of incidence was held constant and the distance between dye layer and the boundary was varied, the opposite was done in related work by CARNIGLIA, MANDEL, DREXHAGE [1972]. Here the fluorescent dye layer was separated from the layer–liquid boundary by a fixed number of 16 CdC_{20} layers providing a distance $d =$ 450 Å. The sample was immersed in Clerici's solution and irradiated with monochromatic light ($\lambda = 476$ nm), polarized perpendicular to the plane of incidence. The fluorescence intensity was recorded as function of the angle of incidence θ. Because the angle α_{fl}, at which the fluorescence was observed, was held constant, the effect described by equation (6.2) was constant throughout the experiment and could be neglected. The experimental plot of I_d versus the angle of incidence θ was found to be in good agreement with the theory, both below and above the critical angle (Fig. 19).

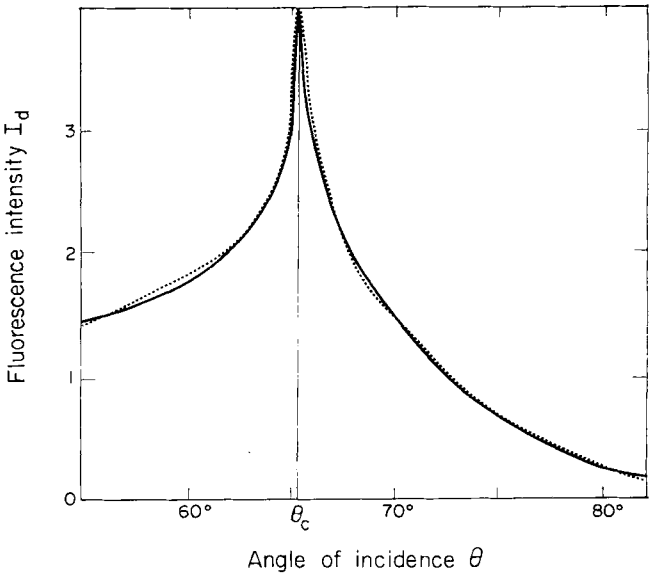

Fig. 19. Evanescent waves: fluorescence intensity I_d ($\sim I_0$) as function of the angle of incidence θ (perpendicular polarization); θ_c critical angle. 16 CdC_{20} cover-layers (d = 450 Å), $\lambda = 476$ nm, $n_1/n_0 = 1.10$. Mixed dye layers (double layers, chromophores face to face) consist of *N,N'*-distearyloxacarbocyanine, *N,N'*-distearylindocarbocyanine and tripalmitin in the ratio 1 : 1 : 16. Experimental values (dots) and theoretical curve (solid). (From CARNIGLIA, MANDEL, DREXHAGE [1972].)

6.2. EVANESCENT WAVES IN A BIREFRINGENT MEDIUM

When the exciting light is polarized perpendicular to the plane of incidence, as was the case in the above experiments, the electric vector of the evanescent wave vibrates perpendicular to the optic axis of the CdC_{20} layers, which then behave like an isotropic medium with refractive index n_0. On the other hand, if the incident light is polarized parallel to the plane of incidence, the birefringence of the CdC_{20} layers must be taken into account. The electric field of the evanescent wave can be derived in a manner analogous to the way in which relation (6.1) is commonly derived. Into the equation for a homogeneous wave, which has been refracted at the boundary between two isotropic dielectrics, are inserted the ray index s of the CdC_{20} layers and the ray refraction angle β. The transition to the case of total reflection is then made in the usual way. With equations (A.3) and (A.5) (see Appendix) the electric-field amplitude (component parallel to surface*) of the evanescent

* The chromophores in the cyanine-dye monolayers, employed in these experiments, are oriented with their transition moments parallel to the surface and respond only to this component of the light field (see § 4).

wave is then given by

$$E_{\parallel} \sim \exp\left[-(2\pi d/\lambda)(n_1^2 \sin^2\theta - n_e^2)^{\frac{1}{2}} n_o n_e^3/(n_e^4 + (n_o^2 - n_e^2) n_1^2 \sin^2\theta)\right]. \quad (6.3)$$

This expression is distinctly different from relation (6.1), to which it reduces for $n_e = n_o$.

It was observed experimentally that for the same angle of incidence θ the decay of $E_{\parallel}$ with the distance d was slower than the decay of $E_{\perp}$ (FORSTER [1967]). This shows directly that the extraordinary refractive index n_e of the CdC_{20} layers is greater than the ordinary index n_o. A comparison of the experimental data with relation (6.3) allows the determination of the extraordinary index, and thus the value $n_e = 1.60 \pm 0.01$ is obtained for $\lambda = 405$ nm.

6.3. EMISSION OF EVANESCENT WAVES

Light emitted from a point source is refracted at the boundary to a more dense medium in such a way that the part entering the dense medium is confined to a cone, the aperture of which is given by the critical angle of total reflection, and no light is found in the region of larger angles. However, if the light source is very close to the boundary, this is no longer true, as was first suggested by SELÉNYI [1913]. By applying the principle of reciprocity he expected that in this case some light should enter the normally dark region just as well, as on reversal of the propagation direction the evanescent wave would cause an absorption by dye molecules that are near the boundary.

This phenomenon has been examined quantitatively with a monomolecular layer of fluorescent dye molecules, separated from the boundary by a certain number of CdC_{20} layers (CARNIGLIA, MANDEL, DREXHAGE [1972]). The experiment was conducted in a manner very similar to the studies of absorption in evanescent waves, which were discussed above. In this case the dye layer was irradiated from the glass side at a constant angle of incidence, and the intensity of the fluorescence emitted into the high-index liquid was recorded as function of the angle θ.

In analogy to relation (6.1) one expects for the fluorescence intensity $I_{\perp}$, emitted into the dense medium at an angle θ greater than the critical angle

$$I_{\perp} \sim \exp\left[-(4\pi d/\lambda)(n_1^2 \sin^2\theta - n_o^2)^{\frac{1}{2}}\right]. \quad (6.4)$$

The experimental data showed that indeed fluorescence was emitted into the region beyond the critical angle in agreement with relation (6.4).

§ 7. The Near Field of a Radiating Molecule

As was mentioned in the introduction, the investigation of radiationless energy transfer between dye molecules was the starting point for the development of the monolayer technique discussed in this article. This phenomenon, which is very important in the field of molecular physics, can be looked upon as absorption in the near zone of an oscillating dipole (the excited molecule). The near field can be probed with a monomolecular layer of another dye in a way similar to § 5 and § 6, where standing and evanescent light waves were examined with such a probe. We will concentrate here on the basic features of the phenomenon and refer to the review articles by KUHN and MÖBIUS [1971] and KUHN [1972] for more details and applications.

7.1. KUHN'S CONCEPT OF ENERGY TRANSFER

If the excited dye molecule is assumed to be a classical oscillating dipole of frequency ν and dipole moment $\mu = \mu_0 \cos 2\pi\nu t$, it will create an electromagnetic field like a radio antenna. At distances $r \ll \lambda$ (λ wavelength of emitted radiation; $\nu = c/\lambda$, where c velocity of light) the amplitude of the alternating electric field, produced by the oscillator, equals the field of a stationary dipole of moment μ_0. Its component E_{DA} along the axis of an acceptor dipole is in first approximation

$$E_{DA} = \mu_0 \kappa_{DA}/n^2 r^3. \tag{7.1}$$

We assume here that the oscillator is surrounded by an isotropic medium of refractive index n. The factor κ_{DA} depends on the relative orientation of the oscillator D (the donor) and the energy acceptor A and is given by $\kappa_{DA} = |\cos\phi_{DA} - 3\cos\phi_D \cos\phi_A|$, where ϕ_{DA} is the angle between the directions of D and A and ϕ_D and ϕ_A denote the angles between the vector from D to A and the direction of D and A, respectively. The energy, absorbed per unit time by the acceptor, is proportional to the square of the local field amplitude E_{DA} and to the absorption coefficient of the acceptor (KUHN [1968, 1970]).

In the case of acceptor molecules arranged in a monomolecular layer, whose absorption at normal incidence for light polarized parallel to the acceptor axes is A, the energy L_a, absorbed per unit time by the layer (area element dS), is given by

$$L_a = (Acn/8\pi)\int E_{DA}^2 \, dS = (A\mu_0^2 c/8\pi n^3)\int (\kappa_{DA}^2/r^6)\, dS.^* \tag{7.2}$$

* Equation (7.2) is restricted to cases in which the absorption properties of the acceptor layer can be expressed in terms of A. An arrangement of acceptor axes perpendicular to the layer plane ($A = 0$) would also show a strong near-field absorption.

In addition to this energy loss the oscillator loses energy by emission of light (fluorescence) and, possibly, by non-radiative (thermal) deactivation processes. The energy loss L_f per unit time due to radiation is given by the well known equation (section 9.1)

$$L_f = 16\pi^4 cn\mu_0^2/3\lambda^4, \tag{7.3}$$

and the contribution L_t of the thermal deactivation is connected with the fluorescence quantum yield q of the molecule in the fluorescent state, the acceptor being absent, by

$$q = L_f/(L_f + L_t). \tag{7.4}$$

It is practical to define a critical distance d_0 between the excited molecule and the acceptor layer, at which the quantity L_a equals the sum of L_f and L_t. This means that at the distance d_0 the probability for energy transfer is equal to the probability for deactivation by any other process.

It follows from equation (7.4) that at the critical distance $L_a = L_f/q$, and by combining equations (7.2) and (7.3) one obtains

$$d_0 = \alpha_{DA}(\lambda/8\pi n)(qA)^{\frac{1}{4}}. \tag{7.5}$$

The factor α_{DA} depends on the mutual orientation of the donor and acceptor molecules, and we may distinguish the following cases:

1) Axis of donor parallel to acceptor layer and

a) acceptor axes in layer plane and parallel to donor axis,

$$\alpha_{DA} = 27^{\frac{1}{4}};$$

b) acceptor axes in layer plane and perpendicular to donor axis,

$$\alpha_{DA} = 9^{\frac{1}{4}};$$

c) acceptor axes randomly distributed in layer plane,

$$\alpha_{DA} = 36^{\frac{1}{4}};$$

d) acceptor axes randomly distributed in space,

$$\alpha_{DA} = 72^{\frac{1}{4}}.$$

2) Axis of donor perpendicular to acceptor layer and

a) acceptor axes randomly distributed in layer plane,

$$\alpha_{DA} = 72^{\frac{1}{4}};$$

b) acceptor axes randomly distributed in space,

$$\alpha_{DA} = 144^{\frac{1}{4}}.$$

TABLE 1

Critical distance d_0 (in Å) according to eqs. (7.5) and (7.11) for $\lambda = 500$ nm, $n = 1.5$ and $q = 1$.

Orientation of donor and acceptor	Absorption A					
	10^{-6}	10^{-5}	10^{-4}	10^{-3}	10^{-2}	10^{-1}
El.-dipole donor						
Case 1, a	10	17	30	54	96	170
b	7	13	23	41	73	129
c	10	18	32	58	103	183
d	12	22	39	69	122	217
Case 2, a	12	22	39	69	122	217
b	15	26	46	82	145	258
El.-quadrup. donor						
Case 1, a	60	89	130	191	281	412
b	46	68	100	146	215	315
c	62	92	134	197	289	425
d	70	103	151	221	325	477
Case 2, a	73	108	158	232	341	500
b	82	121	178	261	383	562

If we assume, for example, donor molecules that fluoresce at $\lambda = 500$ nm with the highest possible quantum yield $q = 1$ and the refractive index $n = 1.5$, we calculate the values of d_0, shown in Table 1 for different orientations and various values of the absorption A. It can be seen that the values of d_0 for an absorption $A = 10^{-2}$, which is typical for a monomolecular dye layer, are about 100 Å corresponding to the thickness of only 4 CdC_{20} layers. Since the quantum yield q is often much smaller than unity, the d_0-values can be markedly smaller in practice.

Equation (7.5) is identical with an equation obtained from Förster's energy-transfer theory (FÖRSTER [1946, 1948]) applied to the case of a layer system and a narrow fluorescence band (DREXHAGE, ZWICK, KUHN [1963]). In the more general case, not limited to a narrow fluorescence band at the wavelength λ, we must, according to Förster's theory, replace in equation (7.5) $\lambda A^{\frac{1}{2}}$ by

$$c\left[\int_0^\infty f_D(\nu)\, A(\nu)\nu^{-4}\mathrm{d}\nu\right]^{\frac{1}{2}},$$

where $f_D(\nu)$ is the normalized quantum spectrum of the fluorescence of D and $A(\nu)$ is the absorption spectrum of the acceptor layer. However, by introducing this refinement the value calculated for d_0 is influenced by only

a few per cent in all practical cases (BÜCHER, DREXHAGE, FLECK, KUHN, MÖBIUS, SCHÄFER, SONDERMANN, SPERLING, TILLMANN, WIEGAND [1967]). It may be mentioned that in case of a highly diluted acceptor layer, where the absorption is not uniformly distributed over the layer, the integration in equation (7.2) is not applicable, and thus the critical distance assumes a value different from the one given by equation (7.5) (BÜCHER, DREXHAGE, FLECK, KUHN, MÖBIUS, SCHÄFER, SONDERMANN, SPERLING, TILLMANN, WIEGAND [1967]).

In the above discussion we have assumed an isotropic dielectric of refractive index n, which is – strictly speaking – not correct, because the CdC_{20} layers are birefringent. This can be taken into account by considering the near field of an oscillating electric dipole in a uniaxial medium, which has been derived by CLEMMOW [1966] p. 159. Taking, for example, the orientation of donor and acceptor molecules corresponding to case 2b, one obtains for the critical distance in analogy to equation (7.5)

$$d_0 = 72^{\frac{1}{4}}(1+n_e^2/n_o^2)^{\frac{1}{4}}(\lambda/8\pi\sqrt{n_o n_e})(qA)^{\frac{1}{4}}. \tag{7.6}$$

It can be inferred from this relation that the neglection of the birefringence in energy-transfer studies is justified, as it introduces only an error of a few percent. We will see later that the experimental error is much larger.

7.2. ENERGY TRANSFER BETWEEN DYE MONOLAYERS

The energy transfer from a layer of fluorescent dye molecules to an absorbing acceptor layer has been investigated in several different ways. As donor molecules cyanine dyes as well as a europium complex have been used, and the near field of these donors was probed by a second dye layer or an evaporated metal film. The dependence of the energy transfer on the separation between donor and acceptor layer was monitored by measuring the fluorescence intensity or decay time of the donor (DREXHAGE and KUHN [1966], BÜCHER, DREXHAGE, FLECK, KUHN, MÖBIUS, SCHÄFER, SONDERMANN, SPERLING, TILLMANN, WIEGAND [1967]) or by following the sensitized fluorescence of the acceptor (MÖBIUS [1969]). From equation (7.2) it follows for the intensity I_d of the donor fluorescence as function of the distance d between donor and acceptor layer

$$I_d/I_\infty = [1+(d_0/d)^4]^{-1}, \tag{7.7}$$

where I_∞ is the fluorescence intensity in the limit $d \to \infty$. The experimental results in the case of energy transfer between two cyanine-dye layers are shown in Fig. 20 together with curves that were calculated according to equation (7.7) with the experimental value of d_0 as parameter (BÜCHER,

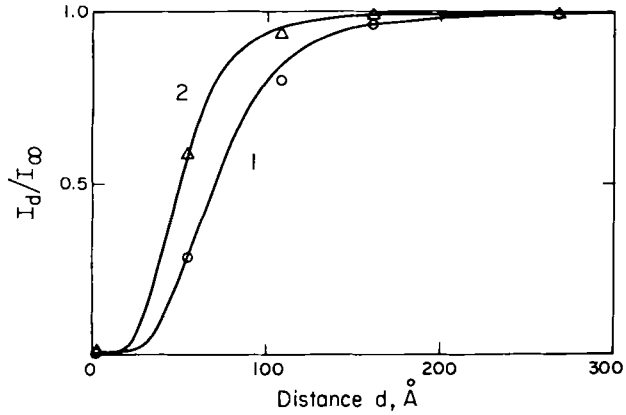

Fig. 20. Energy transfer between dye monolayers. Intensity I_d of donor fluorescence as function of the distance d between donor and acceptor layer. Donor: mixed layer of *N,N'*-distearyloxacyanine and cadmium arachidate in the ratio 1 : 20; acceptor: mixed layer of *N,N'*-distearylthiacyanine and cadmium arachidate in the ratio 1 : 10 (circles) and 1 : 50 (triangles). Curves calculated with eq. (7.7) assuming $d_0 = 70$ Å (curve 1) and $d_0 = 50$ Å (curve 2). (From BÜCHER, DREXHAGE, FLECK, KUHN, MÖBIUS, SCHÄFER, SONDERMANN, SPERLING, TILLMANN, WIEGAND [1967].)

DREXHAGE, FLECK, KUHN, MÖBIUS, SCHÄFER, SONDERMANN, SPERLING, TILLMANN, WIEGAND [1967]).

With respect to these experiments one can adopt two different viewpoints. One may either use the experimental data to verify the theory of energy transfer, or assume the theory to be correct and take any observed deviations as a measure of the regularity of the layer systems. The first view would require an independent verification of the quality of the layers, which has not yet been provided. Since the theory of energy transfer has recently been checked experimentally with an entirely different technique (for example: STRYER and HAUGLAND [1967], HAUGLAND, YGUERABIDE, STRYER [1969]), we may rather adopt the second view and ask ourselves, to which degree irregularities in the layer systems can be ruled out by energy-transfer experiments.

It is to be expected that irregularities in the dye layers cause an apparent increase in the critical distance and a distance dependence of smaller power than given by equation (7.7). Strong deviations of this kind have indeed been observed with dye layers that were prepared by the adsorption technique (§ 2). The value $d_0 = 170$ Å, measured by ZWICK and KUHN [1962], is considerably larger than the highest possible value $d_0 = 52$ Å, obtained from equation (7.5) with $\lambda = 450$ nm, $n = 1.5$, $q = 1$, $A = 10^{-3}$ and $\alpha_{DA} = 36^{\ddagger}$ (case 1c). Likewise, the value $d_0 = 300$ Å, observed experimentally with

similar systems by DREXHAGE, ZWICK, KUHN [1963], is much too large, if compared with the highest possible value $d_0 = 92$ Å, calculated with the same parameters except for $A = 10^{-2}$.

Energy transfer measurements on dye layers that were prepared with the deposition technique generally agree much better with the theoretical predictions. However, the experimental values for the critical distance still tend to be too large. In the case of the experiment of Fig. 20, for example, one calculates from the observed values of d_0 a quantum yield $q = 0.3$, which is markedly higher than the value $q' = 0.05$ obtained by measuring the ratio of emitted quanta to absorbed quanta for a donor layer without the acceptor layer (BÜCHER, KUHN, MANN, MÖBIUS, SZENTPÁLY, TILLMANN [1967]). The quantity q is difficult to determine independently, and in some cases one can escape the conclusion of layer irregularities by making the assumption that the value of q is indeed higher than the quantity q'. Although this is in principle possible, there is no such evidence in the case of the donor molecules studied so far.

Since in most of these layer systems the experimentally observed distance dependence of I_d/I_∞ also shows a slight deviation from equation (7.7) towards a d^{-3}-dependence, the conclusion seems inevitable that these monomolecular dye layers, when examined by the very sensitive energy-transfer test, reveal their limits of regularity. This should present a challenge to workers in the field to further improve the quality of the dye layers. Considering the minute distances involved in the energy-transfer experiments and the rather simple technique of layer preparation, the agreement between theory and experiment is surprisingly good, which suggests that such dye layer systems are very suitable for other optical experiments involving larger characteristic distances.

It may be mentioned that, following an energy transfer, the excitation energy is available to the acceptor for processes like, e.g., fluorescence emission, photochemical reaction, latent image formation, as if the light had been absorbed by the acceptor directly. Thus the weak light absorption of an acceptor can be effectively enhanced owing to strong absorption by a donor and subsequent energy transfer to the acceptor (SZENTPÁLY, MÖBIUS, KUHN [1970]). The upper limit of this enhancement is reached under conditions of complete energy transfer and is given by the absorption ratio of donor and acceptor layer (DREXHAGE [1974]).

7.3. THE NEAR FIELD OF AN ELECTRIC-QUADRUPOLE SOURCE

So far we have considered the energy transfer from a donor, which could be considered as an oscillating electric dipole, to an electric-dipole acceptor

layer. Although this is the most important case, it is possible that light emission originates with an oscillating magnetic dipole or an electric quadrupole. The energy-transfer interaction between one of these and an electric dipole has been considered first by DEXTER [1953], who showed that the probability of energy transfer between el. quadrupole and el. dipole and between magn. dipole and el. dipole decay with the 8th and 4th power of the distance, respectively, as compared with 6th power for el. dipole–el. dipole interaction. In the case of energy transfer between layers the integration analogous to equation (7.2) yields a d^{-6} and a d^{-2}-dependence for el. quadrupole–el. dipole and magn. dipole–el. dipole interaction, respectively. A particularly interesting situation arises, if the donor is an electric-quadrupole oscillator and the acceptor of the electric-dipole type. It is expected theoretically that in this case energy transfer can take place over considerably larger distances than in the familiar case of el. dipole–el. dipole interaction (DREXHAGE [1969], KUHN [1970]).

In order to arrive at this result we may proceed in analogy to section 7.1, and assume as example an axial quadrupole, i.e. an in-line arrangement of two dipoles at a distance δ vibrating in opposite phase with amplitude μ_0. The alternating electric field of the quadrupole is the superposition of the fields of the individual dipoles, and the amplitude E_{QA} of its component along the axis of an acceptor dipole is for $r \ll \lambda$ in first approximation

$$E_{QA} = \delta\mu_0 \kappa_{QA}/n^2 r^4, \tag{7.8}$$

where n is the refractive index of the isotropic medium and r is the distance between donor and acceptor. The orientation factor in this case is $\kappa_{QA} = |6 \cos\phi_{QA} \cos\phi_Q + 3 \cos\phi_A (1\text{-}5 \cos^2\phi_Q)|$. The energy loss per unit time of the quadrupole donor due to light emission is given by

$$L_f = 64\pi^6 c n^3 \delta^2 \mu_0^2 / 15\lambda^6. \tag{7.9}$$

The energy absorbed per unit time by a monomolecular acceptor layer is proportional to E_{QA}^2, and on integration analogous to equation (7.2) one obtains for the intensity of the donor fluorescence

$$I_d/I_\infty = [1+(d_0/d)^6]^{-1}, \tag{7.10}$$

where the critical distance d_0 is

$$d_0 = \alpha_{QA}(\lambda/4\pi n)(qA)^{\frac{1}{6}}. \tag{7.11}$$

The factor α_{QA} depends on the orientation of donor and acceptor transitions

and is in the cases described in section 7.1:

1 a) $\alpha_{QA} = 140.625^{\frac{1}{8}}$; 2 a) $\alpha_{QA} = 450^{\frac{1}{8}}$;

b) $\alpha_{QA} = 28.125^{\frac{1}{8}}$; b) $\alpha_{QA} = 900^{\frac{1}{8}}$.

c) $\alpha_{QA} = 168.75^{\frac{1}{8}}$;

d) $\alpha_{QA} = 337.5^{\frac{1}{8}}$;

If we assume, e.g., the values $\lambda = 500$ nm, $q = 1$ and $n = 1.5$, we obtain the values of d_0 shown in Table 1, and it can be seen that, for a given value of A, they are always greater than in the case of an electric-*dipole* donor. These predictions have not been verified by experiments yet. Finally it may be mentioned that in the case of a magnetic-dipole donor the critical distances are typically smaller than with an electric-dipole donor (INACKER, KUHN, BÜCHER, MEYER, TEWS [1970]).

§ 8. The Radiation Pattern of a Fluorescing Molecule in Front of a Mirror

In the preceding section, the near field of an excited molecule, treated as an optical antenna, has been discussed. In this and the subsequent section experiments will be reviewed, done with the monolayer technique, that involve the interaction of an excited molecule with a mirror. It will be seen that this is again fully analogous to the influence of a reflector on the radiation of a radio antenna. The phenomena to be discussed depend strongly on the orientation of the emitting oscillator and on its nature (electric dipole, quadrupole etc.) and thus can be utilized to obtain such information. The birefringence of the CdC_{20} layers has a marked influence on the results. In this connection, the light emission of a molecule between two reflectors will be discussed.

8.1. THE RADIATION PATTERN IN CASE OF A SINGLE MIRROR AND AN ISOTROPIC MEDIUM

When a fluorescing molecule is placed in front of a mirror, interference between the reflected and unreflected parts of the emitted light wave will occur (Fig. 21). The amplitude of the resultant wave, which depends on the path difference and on the optical properties (phase shift, reflectivity) of the mirror, can be obtained by superposition of the direct and reflected parts of the far field of the oscillator (the excited dye molecule). In the further discussion we will consider besides the familiar electric-dipole oscillator the magnetic dipole and the two electric quadrupoles of Fig. 22. Since the radia-

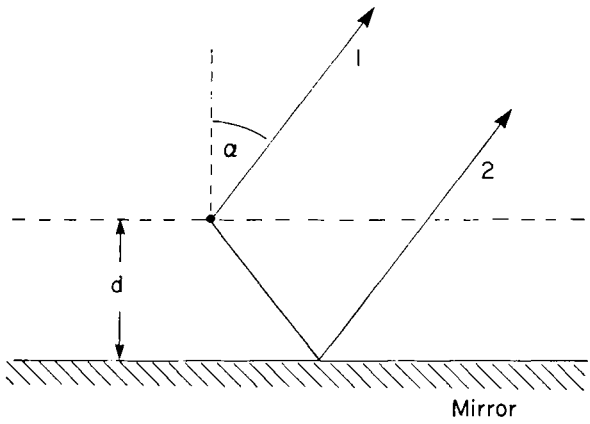

Fig. 21. Fluorescing molecule in front of a mirror. Direct (1) and reflected (2) beams interfere depending on distance d and angle α.

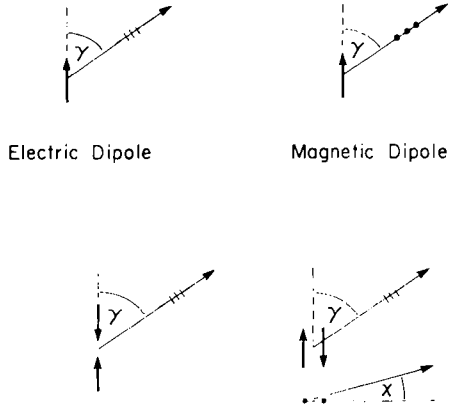

Fig. 22. Molecular oscillators responsible for fluorescence; γ, χ polar coordinates.

tion field is different for each of these sources, one expects different angular patterns of fluorescence also under the influence of a mirror, as was first suggested by SELÉNYI [1911, 1938, 1939]. A more general treatment of wide-angle interference phenomena has been given by HALPERN and DOERMANN [1937], DOERMANN [1938] and DOERMANN and HALPERN [1939].

In the most important case, the electric-dipole oscillator, the electric-field amplitude E_D at a distance $r \gg \lambda$ is given by the well known relation $E_D = B_D \sin \gamma$, where γ is the angle between the dipole axis and the direction of

radiation and B_D is a constant. When placed at a distance d in front of a mirror, the oscillator emits with an intensity proportional to the square of the resultant electric-field amplitude. The patterns of the fluorescence intensity $P_\perp(\alpha)$ (fluorescence polarized perpendicular to plane of incidence) and $P_\parallel(\alpha)$ (parallel polarization), thus obtained, depend on the orientation of the dipole axis relative to the mirror, and we may distinguish the following cases (DREXHAGE, FLECK, KUHN, SCHÄFER, SPERLING [1966], FLECK [1969]).

(1) Electric-dipole axes perpendicular to mirror normal:

$$P_\perp(\alpha) = 1+\rho_\perp^2+2\rho_\perp \cos(\phi-\delta_\perp), \tag{8.1}$$

$$P(\alpha) = \cos^2\alpha\,[1+\rho_\parallel^2+2\rho_\parallel \cos(\phi-\delta)]; \tag{8.2}$$

(2) electric-dipole axes parallel to mirror normal;

$$P_\perp(\alpha) = 0, \tag{8.3}$$

$$P(\alpha) = \sin^2\alpha\,[1+\rho_\parallel^2-2\rho_\parallel \cos(\phi-\delta)]; \tag{8.4}$$

(3) axes of electric dipoles randomly oriented:

$$P_\perp(\alpha) = 1+\rho_\perp^2+2\rho_\perp \cos(\phi-\delta_\perp), \tag{8.5}$$

$$P(\alpha) = 1+\rho_\parallel^2+2\rho_\parallel \cos 2\alpha \cos(\phi-\delta_\parallel). \tag{8.6}$$

Here α is the angle between the mirror normal and the direction of emission and ϕ stands for $4\pi nd\cos\alpha/\lambda$, where n is the refractive index of the environment which is assumed to be isotropic. The quantities $\rho_\perp$ and $\rho_\parallel$ are the reflection coefficients of the mirror and $\delta_\perp$ and δ the phase shifts of the reflected wave for perpendicular and parallel polarization, respectively. These quantities, which depend on the angle of incidence α, can be calculated from the optical constants of the mirror material (see, e.g., BORN and WOLF [1970] p. 615).

The angular dependence of the radiation of a magnetic-dipole oscillator in free space is the same as in the case of an electric dipole (KAUZMANN [1957] p. 614). However, since electric and magnetic field are exchanged (Fig. 23), the radiation pattern of such a source in front of a mirror is different. It can be calculated in the same way, as was outlined above for the electric dipole, and it is found in the case of (DREXHAGE and FLECK [1968], FLECK [1969])

(1) magnetic-dipole axes perpendicular to mirror normal:

$$P_\perp(\alpha) = \cos^2\alpha\,[1+\rho_\perp^2-2\rho_\perp \cos(\phi-\delta_\perp)], \tag{8.7}$$

$$P(\alpha) = 1+\rho_\parallel^2-2\rho_\parallel \cos(\phi-\delta); \tag{8.8}$$

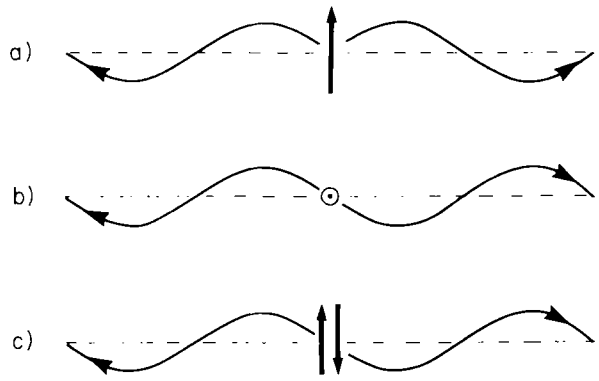

Fig. 23. Phase of electric vector of light waves emitted in opposite directions by a) electric-dipole, b) magnetic-dipole, and c) electric-quadrupole oscillator.

(2) magnetic-dipole axes parallel to mirror normal:

$$P_\perp(\alpha) = \sin^2\alpha\,[1+\rho_\perp^2+2\rho_\perp\cos(\phi-\delta_\perp)], \tag{8.9}$$

$$P_\parallel(\alpha) = 0; \tag{8.10}$$

(3) axes of magnetic dipoles randomly oriented:

$$P_\perp(\alpha) = 1+\rho_\perp^2-2\rho_\perp\cos 2\alpha\cos(\phi-\delta_\perp), \tag{8.11}$$

$$P_\parallel(\alpha) = 1+\rho_\parallel^2-2\rho_\parallel\cos(\phi-\delta_\parallel). \tag{8.12}$$

In the case of the axial electric-quadrupole oscillator of Fig. 22 the electric-field amplitude at distances $r \gg \lambda$ is proportional to $\sin 2\gamma$, where γ is the angle between the axis of the quadrupole and the direction of r (KAUZMANN [1957] p. 611). The radiation pattern of such a source placed at a distance d in front of a mirror is then obtained in the same manner as above (DREXHAGE and FLECK [1968], FLECK [1969]).

(1) Electric-quadrupole axes perpendicular to mirror normal:

$$P_\perp(\alpha) = \sin^2\alpha\,[1+\rho_\perp^2+2\rho_\perp\cos(\phi-\delta_\perp)], \tag{8.13}$$

$$P_\parallel(\alpha) = \tfrac{3}{4}\sin^2 2\alpha\,[1+\rho_\parallel^2+2\rho_\parallel\cos(\phi-\delta_\parallel)]; \tag{8.14}$$

(2) electric-quadrupole axes parallel to mirror normal:

$$P_\perp(\alpha) = 0, \tag{8.15}$$

$$P_\parallel(\alpha) = \sin^2 2\alpha\,[1+\rho_\parallel^2+2\rho_\parallel\cos(\phi-\delta_\parallel)]; \tag{8.16}$$

(3) axes of electric quadrupoles randomly oriented:

$$P_{\perp}(\alpha) = 1+\rho_{\perp}^2-2\rho_{\perp}\cos 2\alpha\cos(\phi-\delta_{\perp}), \tag{8.17}$$

$$P_{\parallel}(\alpha) = 1+\rho_{\parallel}^2-2\rho_{\parallel}\cos 4\alpha\cos(\phi-\delta_{\parallel}). \tag{8.18}$$

In the case of the transversal electric quadrupole of Fig. 22 the electric-field amplitude in the far zone is proportional to $\sin^2\gamma\cos\chi$, where γ and χ are polar coordinates as indicated in Fig. 22. We may distinguish the following principal cases of quadrupole orientation with respect to the mirror.

(1) Electric-quadrupole axes and plane of quadrupoles perpendicular to mirror normal:

$$P_{\perp}(\alpha) = \sin^2\alpha\,[1+\rho_{\perp}^2+2\rho_{\perp}\cos(\phi-\delta_{\perp})], \tag{8.19}$$

$$P_{\parallel}(\alpha) = \tfrac{1}{12}\sin^2 2\alpha\,[1+\rho_{\parallel}^2+2\rho_{\parallel}\cos(\phi-\delta_{\parallel})]; \tag{8.20}$$

(2) electric-quadrupole axes perpendicular, plane of quadrupoles parallel to mirror normal:

$$P_{\perp}(\alpha) = \cos^2\alpha\,[1+\rho_{\perp}^2-2\rho_{\perp}\cos(\phi-\delta_{\perp})], \tag{8.21}$$

$$P_{\parallel}(\alpha) = \cos^4\alpha\,[1+\rho_{\parallel}^2-2\rho_{\parallel}\cos(\phi-\delta_{\parallel})]; \tag{8.22}$$

(3) electric-quadrupole axes parallel to mirror normal:

$$P_{\perp}(\alpha) = 0, \tag{8.23}$$

$$P_{\parallel}(\alpha) = \sin^4\alpha\,[1+\rho_{\parallel}^2-2\rho_{\parallel}\cos(\phi-\delta_{\parallel})]; \tag{8.24}$$

(4) axes of electric quadrupoles randomly oriented:

$$P_{\perp}(\alpha) = 1+\rho_{\perp}^2-2\rho_{\perp}\cos 2\alpha\cos(\phi-\delta_{\perp}), \tag{8.25}$$

$$P_{\parallel}(\alpha) = 1+\rho_{\parallel}^2-2\rho_{\parallel}(\tfrac{5}{8}+\tfrac{3}{8}\cos 4\alpha)\cos(\phi-\delta_{\parallel}). \tag{8.26}$$

It is to be understood here that equations (8.1)–(8.26) represent the *relative* angular dependence of the fluorescence intensity. However, for a given case, the functions $P_{\perp}(\alpha)$ and $P_{\parallel}(\alpha)$ are normalized with respect to each other.

The influence of a mirror on the emission of light is closely related to the absorption in front of a mirror, which was considered in § 5. Both phenomena are reciprocal to each other. Thus equation (8.1) can be derived directly from equation (5.1), which shows that the procedure for obtaining equations (8.1)–(8.26) as outlined above is valid, even though it is based strictly on the *far* zone of the radiation field. Often it is more practical to derive the angular pattern of fluorescence with the help of the reciprocity theorem, in particular, if more than one reflector are involved.

8.2. OBSERVATION OF RADIATION PATTERNS WITH THE MONOLAYER TECHNIQUE

The layer assemblage for the measurement of radiation patterns was similar to the one described in § 5 for the study of standing light waves. A glass plate with a metal coating (e.g., silver or gold) was covered with a certain number of CdC_{20} spacer layers, on top of which a monomolecular layer of the dye to be studied was deposited. In order to avoid the refraction at the layer-air interface as much as possible the sample was placed at the center of a cylindrical cell filled with a liquid whose refractive index matches the index of the layer system (DREXHAGE, FLECK, KUHN, SCHÄFER, SPERLING [1966], DREXHAGE, FLECK, KUHN [1967], DREXHAGE and FLECK [1968], FLECK [1969]). For this purpose nearly saturated aqueous solutions of thallous formate or calcium thiocyanate were used. The latter is preferable, because it is less damaging to the layer systems. In order to protect the dye layer from any chemical attack by the immersion liquid, it was usually covered with 20 or more additional CdC_{20} layers. The sample was irradiated at a fixed angle and the angular distribution of the fluorescence intensity measured.

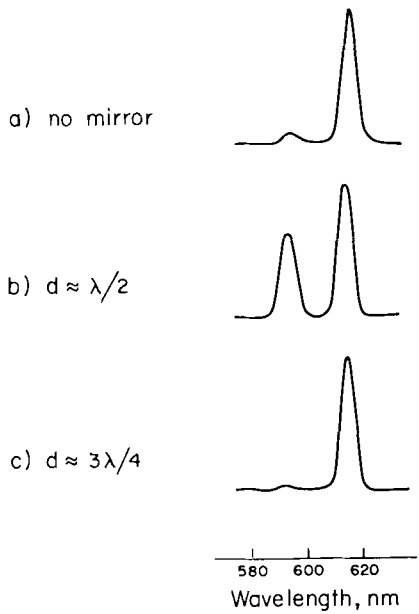

Fig. 24. Fluorescence spectrum of a monomolecular layer of the europium complex of Fig. 4; a) mirror absent, b) and c) in front of gold mirror ($\alpha \approx 0$). Strong dependence of the relative intensities of the fluorescence bands on the distance d shows that the band at 592 nm is *not* electric-dipole in nature. (From DREXHAGE and FLECK [1968].)

The emission of the europium complex of Fig. 4 consists essentially of three relatively narrow bands as shown in Fig. 24. The influence of a mirror on the strongest band (centered around 612 nm) has been studied by FLECK [1969] in great detail. In the case of polarization perpendicular to the plane of incidence, the radiation patterns were found to be in excellent agreement with equation (8.5) for many different distances up to 484 CdC_{20} spacer layers (corresponding to 7 intensity maxima); for two examples see Fig. 25. However, the corresponding patterns for the other polarization (parallel to the plane of incidence) showed marked deviations from $P_{\parallel}(\alpha)$, as given by equation (8.6), and also did not comply with one of the other multipoles (Fig. 27). These deviations, which are particularly pronounced at large angles of incidence, are caused by the birefringence of the layer system and will be discussed further in section 8.4.

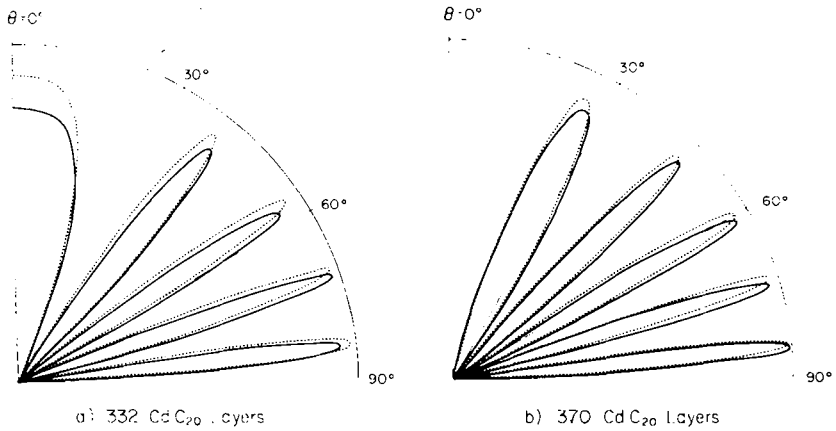

Fig. 25. Fluorescence of europium complex ($\lambda = 612$ nm) in front of gold mirror. Radiation patterns for a) 332 and b) 370 CdC_{20} spacer-layers between mirror and dye layer (mixed double layer; Eu-complex and heptadecyl methyl ketone in the ratio 1 : 2; 20 CdC_{20} cover-layers); immersion liquid with $n_1 = 1.522$; polarization *perpendicular* to plane of incidence ($\alpha = 0$). Experimental data (solid) and theoretical patterns (dashed) calculated with eq. (8.5) using for the gold mirror the optical constants $\nu = 0.505$ and $\nu\kappa = 3.66$. (From FLECK [1969].)

It was shown above that the radiation patterns are quite different for the various possible light sources. This is the case, even if the sources are randomly oriented; compare, e.g., equations (8.6), (8.12), (8.18) and (8.26). A remarkably large difference occurs for emission perpendicular to the mirror ($\alpha = 0$). At certain distances d from the mirror there is either a maximum or minimum of radiation depending on the nature of the emitter, which can be explained in terms of the phase relationship between the waves

emitted in opposite directions (Fig. 23). In the case of the europium complex, a strong dependence of the fluorescence spectrum on the distance from the mirror was observed, indicating that the band at 592 nm is other than electric dipole in nature (Fig. 24). The radiation patterns of this band, isolated by means of an interference filter, were found to be in agreement with the assumption of a magnetic-dipole source (FLECK [1969], DREXHAGE [1970b]), thus confirming an earlier assignment by FREED and WEISSMAN [1941].

The fluorescence and phosphorescence of several cyanine dyes were also examined with this technique (DREXHAGE, FLECK, KUHN [1967], DREXHAGE and FLECK [1968], FLECK [1969]). For polarization perpendicular to the plane of incidence there was full agreement between the measured patterns and equation (8.1) in all cases studied. The interpretation of patterns with parallel polarization is complicated by the birefringence of the CdC_{20} layers. Thus an observation of a small electric-quadrupole contribution in the phosphorescence of a cyanine dye (DREXHAGE and FLECK [1968], FLECK [1969]) needs further confirmation. Owing to the broad luminescence bands of organic dyes (Fig. 5) the radiation patterns differ widely for different parts of the band, giving rise to the colors seen in Fig. 15.

Whereas the monolayer technique provides extremely high resolution, the strong birefringence of the layer systems is certainly a disadvantage compared with the techniques of SELÉNYI [1911, 1938] and KOSSEL [1958]. It seems quite possible, however, that as substitute for cadmium arachidate a material can be found which is less birefringent.

8.3. FLUORESCING MOLECULE BETWEEN TWO MIRRORS

If the layer system is not embedded in an immersion liquid with matching refractive index, the interface between the layers and the surrounding medium has a twofold effect on the angular distribution of the emitted radiation. The outgoing waves are refracted at the interface and, in addition, modified in their intensity by multiple-beam interference. This depends on the reflectivity of the layer surface and hence is particularly pronounced at large angles of incidence. To calculate the angular pattern $\bar{P}(\theta)$ of the fluorescence emitted by a molecule between two reflectors, one may apply the reciprocity principle, i.e. determine the absorption of an absorber molecule in place of the emitter as function of the angle of incidence θ. The local electric-field amplitude is found by superposition of all partial waves (FLECK [1969], see also KOPPELMANN [1969] p. 8).

In the case of polarization perpendicular to the plane of incidence one thus obtains for the angular pattern

$$\bar{P}_\perp(\theta) = P_\perp(\alpha) t_{12}^{\perp 2} / [1 + \rho_\perp^2 r_{21}^{\perp 2} - 2\rho_\perp r_{21}^\perp \cos(4\pi n_0 (d+d') \cos\alpha/\lambda - \delta_\perp)]. \quad (8.27)$$

Here $\rho_\perp$ and $\delta_\perp$ are reflection coefficient and phase shift of the underlying metal mirror, respectively. The reflection coefficient $r_{21}^\perp$ and the transmission coefficient $t_{12}^\perp$ of the dielectric interface are given by Fresnel's formulas (BORN and WOLF [1970] p. 40)*:

$$r_{21}^\perp = (n_0 \cos\alpha - n_1 \cos\theta)/(n_0 \cos\alpha + n_1 \cos\theta); \quad (8.28)$$

$$t_{12}^\perp = 2n_1 \cos\theta/(n_1 \cos\theta + n_0 \cos\alpha). \quad (8.29)$$

The quantity d' is the distance between the emitter and the layer surface, and $P_\perp(\alpha)$ represents the radiation pattern in the case of a single reflector, the metal mirror (see section 8.1). The angles α and θ are connected by Snell's law: $n_0 \sin\alpha = n_1 \sin\theta$. In case of exact index matching ($n_0 = n_1$; $r_{21}^\perp = 0$) the quantities $P_\perp(\alpha)$ and $\bar{P}_\perp(\theta)$ are identical.

According to equation (8.27) the pattern $\bar{P}_\perp(\theta)$ is dependent on the distance d'. This was confirmed experimentally by FLECK [1969] on samples that were not immersed in any liquid and carried a varying number of CdC_{20} cover layers, while the distance d and $P(\alpha)$ were held constant (Fig. 26). The experimental results were found to be in full agreement with equation (8.27).

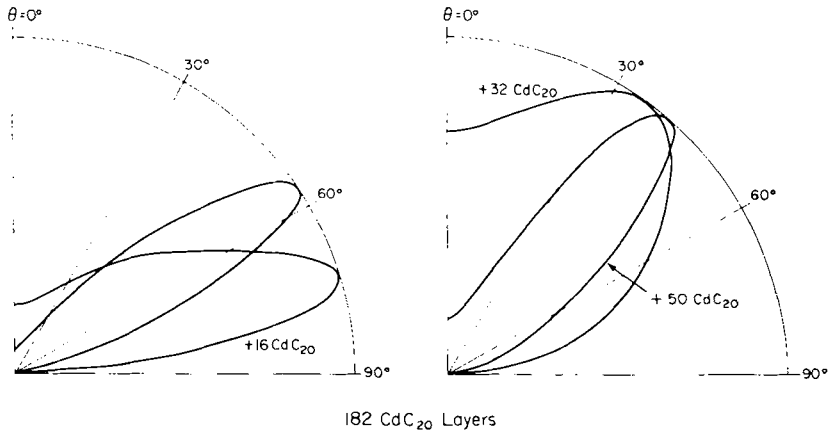

Fig. 26. Fluorescence of a cyanine dye (λ = 525 nm) in front of silver mirror. Observed radiation patterns for 182 CdC_{20} spacer-layers between mirror and dye layer (mixed double layer; *N,N'*-distearylthiacyanine and cadmium arachidate in the ratio 1 : 10); no immersion liquid; polarization perpendicular to plane of incidence. Angular pattern depends on the number of cadmium arachidate cover-layers (left: 0, +16; right: +32, +50). (From FLECK [1969].)

* It may be mentioned that in case of $n_1 > n_0$ equations (8.27) and (8.30) are invalid at those angles θ at which emission of evanescent waves occurs (§ 6).

If the difference $n_1 - n_0$ is very small, the reflection coefficient $r_{21}^{\perp}$ is also small, and thus the multiple-beam interference is negligible. In this case the dielectric interface causes only a refraction of the pattern $P_{\perp}(\alpha)$,* which can be utilized to determine the refractive index of the layer system. For this purpose the position of a fluorescence maximum (preferably at large angle θ) is measured in an immersion liquid with a refractive index n_1 very close to n_0 and the result is compared with the position to be expected from equation (8.5). Making use of Snell's law the unknown index n_0 can then be calculated. At larger differences $n_1 - n_0$ equation (8.27) must be used. With this method FLECK [1969] obtained for CdC_{20} layers at $\lambda = 612$ nm the value $n_0 = 1.522$ and similarly for the extraordinary index the value $n_e = 1.59$ (see section 8.4).

8.4. THE INFLUENCE OF THE LAYER BIREFRINGENCE

The angular patterns of the fluorescence polarized *parallel* to the plane of incidence are inevitably affected by the birefringence of the CdC_{20} layers. It is not possible to match the refractive index of the layers with an immersion liquid for all angles of incidence. If, e.g., the refractive index n_1 of the liquid is chosen to match the ordinary index n_0 of the layers, a marked mismatch will occur at large angles of incidence, and the radiation patterns observed experimentally deviate considerably from those expected according to section 8.1 (BÜCHER, DREXHAGE, FLECK, KUHN, MÖBIUS, SCHÄFER, SONDERMANN, SPERLING, TILLMANN, WIEGAND [1967], FLECK [1969]).

To account for the influence of the layer–liquid interface one can proceed in a manner analogous to section 8.3 and obtains for the angular pattern $\bar{P}_{\parallel}(\theta)$ of the fluorescence polarized parallel to the plane of incidence

$$\bar{P}_{\parallel}(\theta) = F_{\parallel}(\beta) t_{12}^{\parallel 2} / [1 + \rho_{\perp}^2 \, r_{21}^{\parallel 2} - 2\rho_{\perp} \, r_{21}^{\parallel} \cos(4\pi n_0^2 (d + d') \cos\beta / s\lambda - \delta_{\perp})]. \tag{8.30}$$

The reflection coefficient $\rho_{\parallel}$ and the phase shift $\delta_{\parallel}$ of the underlying mirror are functions of the angle of incidence β of the ray. The function $F_{\parallel}(\beta)$ is obtained from equations (8.2), (8.4) etc., if one replaces the factors $\cos^2\alpha$, $\sin^2\alpha$, etc. by $\cos^2\beta$, $\sin^2\beta$, etc. and the quantity ϕ by $4\pi n_0^2 d \cos\beta / s\lambda$. For instance, in the case of randomly oriented electric-dipoles one finds so from equation (8.6)

$$F_{\parallel}(\beta) = 1 + \rho_{\parallel}^2 + 2\rho_{\parallel} \cos 2\beta \cos(4\pi n_0^2 d \cos\beta / s\lambda - \delta_{\parallel}).$$

* The effect of slight variations in the refractive index n_0 on the fluorescence pattern $P_{\perp}(\alpha)$ is negligible at large angles α.

The reflection coefficient $r_{21}^{\parallel}$ and the transmission coefficient $t_{12}^{\parallel}$ of the dielectric interface are given by equations (A.9) and (A.10). The ray index s is connected with the angle β by $s^2 = n_o^2 \cos^2\beta + n_e^2 \sin^2\beta$, and the refraction is expressed by $n_1 s \sin\theta = n_e^2 \sin\beta$ (see Appendix).

It follows from equation (8.30) that the pattern $\bar{P}_{\parallel}(\theta)$ depends in any case on the total thickness $d+d'$ of the layer system, i.e. in practice on the number of CdC_{20} layers covering the fluorescent dye layer. This is in contrast to the case of perpendicular polarization, where the influence of the layer surface can be eliminated completely through the proper choice of the immersion liquid. The above treatment was found to be in good agreement with fluorescence patterns measured on the europium complex by FLECK [1969]. A typical example for the influence of the birefringence is shown in Fig. 27, where the patterns $P_{\parallel}(\alpha)$, calculated with equation (8.6), are compared with the experimentally observed patterns $\bar{P}_{\parallel}(\theta)$.

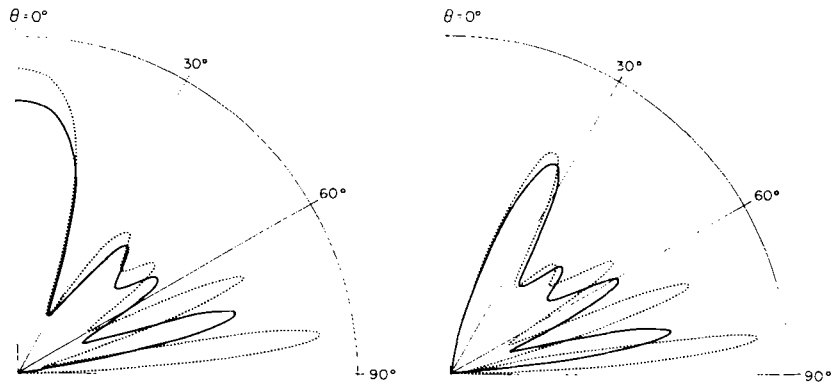

Fig. 27. Fluorescence of europium complex ($\lambda = 612$ nm) in front of gold mirror. Observed radiation patterns (solid) for a) 332 and b) 370 CdC_{20} spacer-layers between mirror and dye layer (same as in Fig. 25); immersion liquid with $n_1 = 1.522$; polarization *parallel* to plane of incidence. Functions $P_{\parallel}(\alpha)$ (dashed) calculated with eq. (8.6) using the optical constants $\nu = 0.505$ and $\nu\kappa = 3.66$. (From FLECK [1969].)

§ 9. Fluorescence Decay Time of a Molecule in Front of a Mirror

It is well known that the radiation resistance of an antenna depends on the environment and in particular on the presence of reflecting surfaces. By analogy one should expect such an effect also in case of a radiating atom or molecule, where it would manifest itself in an influence of the reflector on the decay time of fluorescence. This has indeed been observed for the first time with the aid of the monolayer technique (DREXHAGE, FLECK, KUHN,

SCHÄFER, SPERLING [1966]). All experiments concerning this phenomenon have been carried out on the europium complex of Fig. 4, which exhibits a narrow and strong fluorescence band and a conveniently long decay time (about 1 msec). It will be seen that the experimental results can be understood very well in terms of a classical theory. Some slight deviations are possibly due to the birefringence of the layer systems, which has not been taken into account.

9.1. ELECTRIC-DIPOLE OSCILLATOR IN FRONT OF A SINGLE MIRROR

An oscillating electric dipole (the excited molecule) in free space will create an electromagnetic wave, whose electric-field amplitude at a distance $r \gg \lambda$ is given by (compare section 8.1)

$$E_D = (4\pi^2\mu_0/\lambda^2 r)\sin\gamma. \tag{9.1}$$

The total energy L_f, emitted by such an oscillator per unit time, is obtained by integration over all angles,

$$L_f = \frac{cn}{8\pi}\int_0^{\pi}\int_0^{2\pi} E_D^2 r^2 \sin\gamma\,d\gamma\,d\psi = 16\pi^4 cn\mu_0^2/3\lambda^4. \tag{7.3}$$

This expression serves here as a measure for the radiation rate of the excited molecule, in that we assume $1/\tau \sim L_f$ where τ is the radiative decay time of the molecule.

If we now place this oscillator in front of a reflector, the electric field in the far zone is no longer given by equation (9.1), but is obtained by superposition of the direct and reflected waves instead. The angular distribution of the radiation is strongly dependent on the distance d from the mirror and on the orientation of the oscillator (section 8.1). In case of the dipole axis being parallel to the mirror normal the electric-field amplitude $E_{D,M}^{\parallel}$ is given by (compare equation (8.4))

$$E_{D,M}^{\parallel} = (4\pi^2\mu_0/\lambda^2 r)\sin\alpha\,[1+\rho_{\parallel}^2-2\rho_{\parallel}\cos(4\pi nd\cos\alpha/\lambda-\delta_{\parallel})]^{\frac{1}{2}} \tag{9.2}$$

where α is the angle of incidence on the mirror and n is the refractive index of the medium, which is assumed to be isotropic. If the reflectivity of the mirror is less than unity ($\rho_{\parallel} < 1$) owing to transmission, there will also be a wave beyond the mirror with the amplitude

$$\bar{E}_{D,M}^{\parallel} = (4\pi^2\mu_0/\lambda^2 r)\sin\alpha\,(1-\rho_{\parallel}^2)^{\frac{1}{2}}. \tag{9.3}$$

The total energy $L_{f,M}$, radiated per unit time, is therefore

$$L_{f,M} = \frac{cn}{8\pi}\int_0^{\pi/2}\int_0^{2\pi}(E_{D,M}^2 + \bar{E}_{D,M}^2)r^2 \sin\alpha\, d\alpha\, d\psi.^* \tag{9.4}$$

Through the substitutions $z = 4\pi nd/\lambda$ and $u = \cos\alpha$ and with equations (9.2) and (9.3) one obtains for the power, radiated by the oscillator in front of the mirror,

$$L_{f,M}^{\parallel} = (16\pi^4 cn\mu_0^2/3\lambda^4)\left[1 - \tfrac{3}{2}\int_0^1 \rho_{\parallel}(1-u^2)\cos(zu-\delta_{\parallel})du\right]. \tag{9.5}$$

The quantity $L_{f,M}^{\parallel}$ is proportional to $1/\tau_M^{\parallel}$ ($\tau_M^{\parallel}$ radiative decay time of the molecule under the influence of the mirror), and with equation (7.3) one finds (DREXHAGE [1966, 1970a])

$$\tau/\tau_M^{\parallel} = 1 - \tfrac{3}{2}\int_0^1 \rho_{\parallel}(1-u^2)\cos(zu-\delta_{\parallel})du. \tag{9.6}$$

In the case of the dipole axis being perpendicular to the mirror normal one obtains correspondingly for the decay-time ratio

$$\tau/\tau_M^{\perp} = 1 + \tfrac{3}{4}\int_0^1 [\rho_{\perp}\cos(zu-\delta_{\perp}) + \rho_{\parallel}u^2\cos(zu-\delta_{\parallel})]\,du. \tag{9.7}$$

It is seen from equations (9.6) and (9.7) that the decay-time ratio depends on the distance d and, in particular, on the optical properties of the mirror, i.e. on the reflection coefficients $\rho_{\parallel}$, $\rho_{\perp}$ and the phase shifts $\delta_{\parallel}$, $\delta_{\perp}$ as functions of the angle α. If one assumes for the sake of simplicity $\rho_{\parallel} = \rho_{\perp} = 1$ and $\delta_{\parallel} = \delta_{\perp} = \pi$, independent of α, the integration can be carried out in closed form, and one obtains the following results (DREXHAGE, FLECK, KUHN, SCHÄFER, SPERLING [1966]), which are in agreement with a different theoretical treatment by MORAWITZ [1969]:

$$\tau/\tau_M^{\parallel} = 1 - 3z^{-2}\cos z + 3z^{-3}\sin z; \tag{9.8}$$

$$\tau/\tau_M^{\perp} = 1 - \tfrac{3}{2}z^{-1}\sin z - \tfrac{3}{2}z^{-2}\cos z + \tfrac{3}{2}z^{-3}\sin z. \tag{9.9}$$

However, such optical properties are not found with any *real* mirror. For instance, in case of a highly reflecting metal mirror there is a strong dependence, in particular, of the quantity $\delta_{\parallel}$ on the angle of incidence α, which results in decay-time functions quite different from equations (9.8) and (9.9)

* The effect of a mirror with $\rho_{\parallel} < 1$ on the oscillator is the same, whether the reduced reflectivity is caused by transmission or absorption in the mirror. Thus equation (9.4) is valid also in the case of an absorbing mirror (e.g., silver or gold).

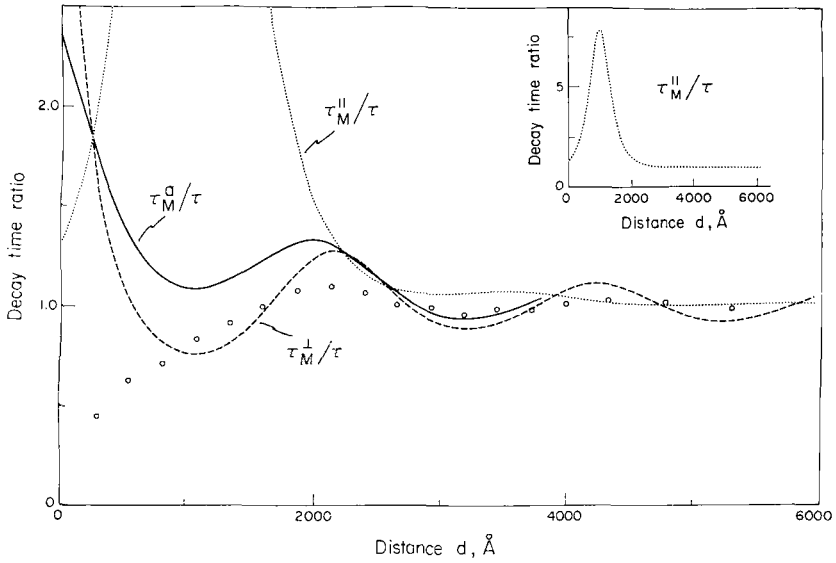

Fig. 28. Fluorescence decay time of europium complex as function of the distance d between dye and a gold mirror. Experimental data (circles) obtained on a mixed double layer of Eu-complex and tripalmitin in the ratio 1 : 3; 40 CdC_{20} cover-layers, immersion liquid with $n_1 = 1.52$. Theoretical plots of $\tau_M^{\parallel}/\tau$ (dotted), $\tau_M^{\perp}/\tau$ (dashed), and τ_M^{a}/τ (solid) calculated with eqs. (9.6), (9.7) and (9.10) using for the gold mirror the optical constants $\nu = 0.505$ and $\nu\kappa = 3.66$. (From DREXHAGE [1966] and unpublished results.)

(Fig. 28). Since the experiments were done on monolayers of the europium complex, where the fluorescing central atom is uniformly surrounded by the ligands so that the transition moment does not have a preferred orientation, the expected decay time τ_M^a is given by the average

$$1/\tau_M^a = \tfrac{1}{3}(1/\tau_M^{\parallel}) + \tfrac{2}{3}(1/\tau_M^{\perp}). \tag{9.10}$$

The samples for these measurements were prepared according to § 2 and § 8. The fluorescence was excited with ultraviolet light from a high-pressure mercury arc, which was chopped by a rotating disc into pulses with a sharp cutoff. The intense fluorescence ($\lambda \approx 612$ nm) was detected by a photomultiplier tube and recorded by a sampling technique. The decay was usually found to be exponential over two decades, if the precautions for the layer deposition, outlined in § 2, were met. Some results on samples with a gold mirror are shown in Fig. 28. In order to avoid reflection at the surface of the layer systems as much as possible, the samples were immersed in a liquid of refractive index $n_1 = 1.52$ (thallous formate in water). While a variation of the decay time with distance d was observed in qualitative accord with

the above theory, it was not as pronounced as expected. This was found with all mirror systems studied and can be ascribed to the influence of competing nonradiative processes (section 9.4). The considerable deviations occurring at small distances are caused by energy transfer to the absorbing metal film (§ 7), whose probability rises sharply with decreasing distance d. This additional deactivation mechanism, which shortens the decay time, was not included in the above theory. It is absent with a dielectric interface as reflector (section 9.2).

The influence of a metal mirror on the decay time of an excited molecule has also been treated by introducing into the equation of motion of a classical harmonic oscillator the force, which is exerted on the oscillator by the wave reflected at the mirror (KUHN [1970]). Since the phase with which the reflected wave (the "echo") returns to the oscillator depends on the distance d and on the value of δ (at normal incidence), the decay time of fluorescence will depend on these parameters. While the problem was not solved rigorously for arbitrary values of ρ and δ, the following approximative expressions have been derived:

$$\tau/\tau_M^{\parallel} = 1+3\rho[z^{-2}\cos(z-\delta)-z^{-3}\sin(z-\delta)]; \tag{9.11}$$

$$\tau/\tau_M^{\perp} = 1+\tfrac{3}{2}\rho[z^{-1}\sin(z-\delta)+z^{-2}\cos(z-\delta)-z^{-3}\sin(z-\delta)]. \tag{9.12}$$

They are strictly valid for $z \gg 1$ and cannot be applied to cases like, e.g., the reflecting interface between two transparent media*. Whereas the values of $\tau_M^{\perp}$, so obtained, are in general comparable with those, given by equation (9.7), there is a serious discrepancy between the values of $\tau_M^{\parallel}$ calculated with equations (9.6) and (9.11). The energy transfer to the absorbing mirror is naturally included in this approach. Both this treatment and the one by MORAWITZ [1969] predict also a shift of the oscillator frequency near the mirror, which has not yet been observed experimentally.

9.2. DIELECTRIC INTERFACE AS MIRROR

The influence of a reflector on the radiation resistance of a fluorescing molecule, as treated in section 9.1, is expected to occur with any kind of reflecting surface. If its optical properties are known, the decay times $\tau_M^{\parallel}$ and $\tau_M^{\perp}$ can be calculated from equations (9.6) and (9.7). In the case of an interface between transparent dielectrics of different refractive index the reflection coefficient is given by Fresnel's formulas (BORN and WOLF [1970] p. 40):

$$r_{21}^{\perp} = (n\cos\alpha - n_1\cos\theta)/(n\cos\alpha + n_1\cos\theta); \tag{9.13}$$

$$r_{21}^{\parallel} = (n\cos\theta - n_1\cos\alpha)/(n\cos\theta + n_1\cos\alpha). \tag{9.14}$$

* H. Kuhn, private communication.

These equations apply at angles of incidence α smaller than the critical angle of total reflection. The phase information is contained in the sign of $r_{21}^{\perp}$ and $r_{21}^{\parallel}$. In the range of total reflection, however, the phase shift is given by*

$$\tan\left(\tfrac{1}{2}\delta_{21}^{\perp}\right) = (n^2 \sin^2\alpha - n_1^2)^{\frac{1}{2}}/n\cos\alpha; \tag{9.15}$$

$$\tan\left[\tfrac{1}{2}(\delta_{21}^{\parallel}+\pi)\right] = n(n^2\sin^2\alpha - n_1^2)^{\frac{1}{2}}/n_1^2\cos\alpha. \tag{9.16}$$

Here n denotes the refractive index of the layers, which are assumed to be isotropic, and n_1 is the refractive index of the second dielectric. The angles α and θ are connected by Snell's law, $n\sin\alpha = n_1\sin\theta$. The decay times $\tau_M^{\parallel}$, $\tau_M^{\perp}$ and τ_M^{a}, calculated with equations (9.13) to (9.16) for $n = 1.54$ and $n_1 = 1$ (air), are shown as functions of the distance d in Fig. 29 (DREXHAGE[1970a]).

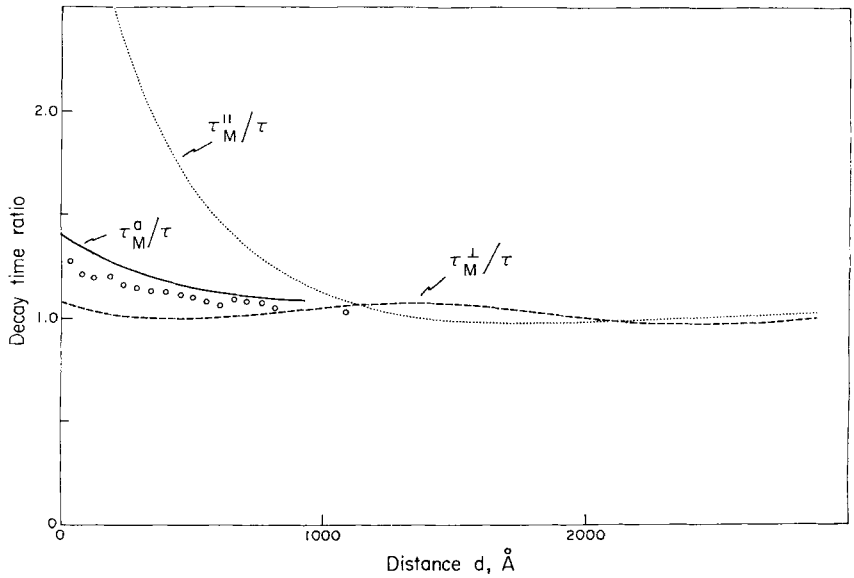

Fig. 29. Fluorescence decay time of europium complex as function of the distance d between dye and layer surface. Experimental data (circles) obtained on a mixed double layer of Eu-complex and tripalmitin in the ratio 1 : 3 with varying number of CdC_{20} coverlayers. Theoretical plots of $\tau_M^{\parallel}/\tau$ (dotted), $\tau_M^{\perp}/\tau$ (dashed), and τ_M^{a}/τ (solid) calculated with eqs. (9.6), (9.7), (9.10) and (9.13) to (9.16) using $n = 1.54$ and $n_1 = 1$. (From DREXHAGE [1970a].)

In the case of electric dipoles located directly at the interface ($d = 0$) the integration in equations (9.6) and (9.7) can be carried out in closed form,

* For the method of calculation see BORN and WOLF [1970] p. 49. The formulas given there are slightly different owing to different definitions of the phase shifts.

and it is obtained with $n/n_1 = a$ (DREXHAGE [1972])

$$\tau/\tau_M^{\parallel} = \frac{a^3+2a^2-2a-1-3a^2(a^2+1)^{-\frac{1}{2}}\ln\left[a-1+a^{-1}+(a^{-1}-1)(a^2+1)^{\frac{1}{2}}\right]}{a^7+a^5-a^3-a} \tag{9.17}$$

and

$$\tau/\tau_M^{\perp} = \frac{a^7+\frac{3}{2}a^5-2a^4+2a^3-\frac{3}{2}a^2-1+\frac{3}{2}a^4(a^2+1)^{-\frac{1}{2}}\ln\left[a-1+a^{-1}+(a^{-1}-1)(a^2+1)^{\frac{1}{2}}\right]}{a^7+a^5-a^3-a}. \tag{9.18}$$

These equations, which are valid for any value of a,* describe the radiation rate of atoms or molecules adsorbed at an interface, a situation of particular practical importance. By substituting $1/a$ for a it is found that $\tau_M^{\perp}$ is identical for a radiating molecule on either side of the interface, whereas $\tau_M^{\parallel}$ changes by the factor a^4, as the molecule crosses the interface from the medium with index n_1 into the medium with index n.** Both results might be expected, since the tangential component of the electric field and the normal component of the electric displacement must be continuous across the interface (BORN and WOLF [1970] p. 4). The change in decay time is expected to be most pronounced, if the fluorescing molecule is directly at the interface. We obtain, e.g., with $a = 1.54$ the values $\tau_M^{\parallel}/\tau = 3.60$ and $\tau_M^{\perp}/\tau = 1.08$, and with $a = 2.00$ the values $\tau_M^{\parallel}/\tau = 9.28$ and $\tau_M^{\perp}/\tau = 1.05$.

The above derivation of the decay time for any distance d is entirely based on the *far* field of oscillating electric dipoles. The validity of this procedure may be doubted for small distances d. However, identical expressions for the decay time are obtained by application of the reciprocity theorem, where such objections do not apply, because the behavior of standing light waves is well understood for any distance d from the reflector (§ 5).

A theoretical treatment, entirely different from the above, considers the induced dipoles in the material surrounding the excited molecule and the field produced by these dipoles at the site of the oscillator (TEWS, INACKER, KUHN [1970]). Depending on the phase relation between the induced field

* In the case $n < n_1$ the emission of evanescent waves must be taken into account in equations (9.6) and (9.7) (see section 6.3).

** At large distance from the mirror the radiative decay time τ of an electric-dipole oscillator in a medium of index n equals τ_{vac}/n, where τ_{vac} is the decay time in vacuo (compare equation (7.3)).

and the motion of the oscillator it is accelerated or slowed down, and thus the decay time will be shortened or increased. The interaction between induced dipoles is neglected, and the following expressions are obtained:

$$\frac{\tau}{\tau_M^{\parallel}} = 1 + \frac{9}{8n^2}\,\frac{n_1^2-n^2}{2n_1^2+n^2}\left[\cos z + \frac{\sin z}{z} - \frac{4\cos z}{z^2} + \frac{4\sin z}{z^3} + z(\mathrm{Si}(z)-\tfrac{1}{2}\pi)\right] \tag{9.19}$$

and

$$\frac{\tau}{\tau_M^{\perp}} = 1 + \frac{9}{16n^2}\,\frac{n_1^2-n^2}{2n_1^2+n^2}\left[\cos z - \frac{\sin z}{z} - \frac{4\cos z}{z^2} + \frac{4\sin z}{z^3} + z(\mathrm{Si}(z)-\tfrac{1}{2}\pi)\right]. \tag{9.20}$$

These results differ considerably from equations (9.6) and (9.7), applied to a dielectric interface as mirror, in particular for an oscillator oriented parallel to the mirror normal. For instance, at the distance $d = 0$ one obtains with $n = 1.54$ and $n_1 = 1.00$ the value $\tau_M^{\parallel}/\tau = 1.98$ and with $n = 2.00$ and $n_1 = 1.00$ the value $\tau_M^{\parallel}/\tau = 1.88$. The discrepancies are most likely due to the approximations on which equations (9.19) and (9.20) are based.

Experimentally only the interface between the layer systems and air has been studied as reflector. A monolayer of the europium complex, deposited on a glass plate on top of, say, 5 CdC_{20} layers, was covered with a varying number of CdC_{20} or tripalmitin layers, and the decay time of the red fluorescence was measured as a function of the distance between the dye layer and the interface (DREXHAGE [1970a], TEWS, INACKER, KUHN [1970]). The results (Fig. 29) do not show a particularly pronounced distance dependence of the decay time and agree with equations (9.6) and (9.7) assuming a quantum yield $q = 0.7$ and with equations (9.19) and (9.20) under the assumption $q = 1.0$ (section 9.4).

9.3. ELECTRIC-DIPOLE SOURCE BETWEEN TWO MIRRORS

The gradual decrease of the fluorescence decay time with the distance d observed in the studies of section 9.2 does not prove an influence of the reflector on the decay time, although it was found to be in agreement with the predictions. Such a decrease of the decay time, in principle, could be caused equally well by an enhancement of competing non-radiative processes due to the cover layers. Likewise, an immersion liquid might reduce the decay time through a chemical attack on the very sensitive europium complex. But a very pronounced and unambiguous mirror effect has been observed using a highly reflecting metal mirror, which was covered only with a varying number of CdC_{20} layers and a monolayer of the europium com-

plex, avoiding any additional treatment. Unfortunately, the interface between the layers and air constitutes an additional reflector, which needs to be accounted for in the theoretical treatment.

The theory, discussed in section 9.1, can be extended in a straightforward way to the case of an emitter between two mirrors. It is presumed as before that the metal mirror (reflection coefficients $\rho_\perp$, $\rho_\parallel$; phase shifts $\delta_\perp$, $\delta_\parallel$) acts upon the oscillator like a nonabsorbing mirror with the transmission coefficients $(1-\rho_\perp^2)^{\frac{1}{2}}$ and $(1-\rho_\parallel^2)^{\frac{1}{2}}$. Then the radiation pattern on either side of the layer system can be calculated, taking into account the multiple-beam interference as was outlined in section 8.3. The total energy, radiated per unit time, is obtained in analogy to equation (9.4), and with equation (7.3) the following expressions for the decay-time ratios are found:

$$\frac{\tau}{\tau_M} = \tfrac{3}{2}\int_0^1 \frac{1-\rho^2\, r_{21}^{\parallel 2} - (1-r_{21}^{\parallel 2})\rho_\parallel \cos(zu-\delta_\parallel) - (1-\rho_\parallel^2) r_{21}^{\parallel} \cos(z'u-\delta_{21}^{\parallel})}{1+\rho^2\, r_{21}^{\parallel 2} - 2\rho\; r_{21}^{\parallel} \cos(zu+z'u-\delta\; -\delta_{21}^{\parallel})} \times (1-u^2)\,du; \quad (9.21)$$

$$\frac{\tau}{\tau_M^\perp} = \tfrac{3}{4}\int_0^1 \left[\frac{1-\rho_\parallel^2\, r_{21}^{\parallel 2} + (1-r_{21}^{\parallel 2})\rho\; \cos(zu-\delta\;) + (1-\rho_\parallel^2) r_{21}^{\parallel} \cos(z'u-\delta_{21}^{\parallel})}{1+\rho_\parallel^2\, r_{21}^{2} - 2\rho_\parallel\; r_{21}^{\parallel} \cos(zu+z'u-\delta_\parallel-\delta_{21}^{\parallel})} u^2 + \frac{1-\rho_\perp^2 r_{21}^{\perp 2} + (1-r_{21}^{\perp 2})\rho_\perp \cos(zu-\delta_\perp) + (1-\rho_\perp^2) r_{21}^{\perp} \cos(z'u-\delta_{21}^{\perp})}{1+\rho_\perp^2 r_{21}^{\perp 2} - 2\rho_\perp r_{21}^{\perp} \cos(zu+z'u-\delta_\perp-\delta_{21}^{\perp})}\right] du. \quad (9.22)$$

The reflection coefficients $r_{21}^{\perp}$, $r_{21}^{\parallel}$ and the phase shifts $\delta_{21}^{\perp}$, $\delta_{21}^{\parallel}$ of the dielectric interface are given by equations (9.13) to (9.16), whereas those quantities for the metal mirror can be calculated from the optical constants of the mirror material in the usual manner (BORN and WOLF [1970] p. 615). The quantity z' stands for $4\pi nd'/\lambda$, where d' denotes the distance between the fluorescing molecule and the dielectric interface. Furthermore it is assumed $n > n_1$ so that no emission of evanescent waves occurs. Equations (9.21) and (9.22) reduce to equations (9.6) and (9.7) for $n_1 = n$ ($r_{21}^{\perp} = r_{21}^{\parallel} = 0$).

Of particular interest is again the decay time τ_M^a, which is obtained with equation (9.10). It has been calculated as a function of distance d for the experimentally relevant case of a silver mirror and the parameters $n = 1.54$,

$n_1 = 1$, $d' = 0$ and $\lambda = 612$ nm by DREXHAGE [1970a, b]*. The ratio of the decay time $\tau_M^a(d)$ so obtained and the decay time $\tau_M^a(\infty)$, which is calculated from equations (9.17), (9.18) and (9.10), is shown for a gold mirror in Fig. 30. The layer–air interface, acting as a second reflector, gives rise to a generally more pronounced variation of the decay time than is caused by the gold mirror alone (compare Fig. 28). This is also true for other mirror materials, e.g. silver, copper or aluminium.

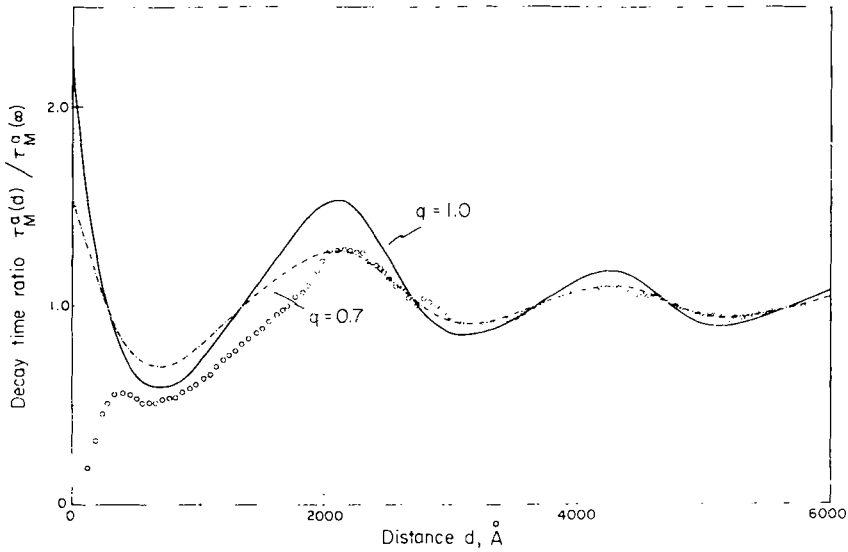

Fig. 30. Fluorescence decay time of europium complex between gold mirror and layer surface as function of the separation d from the mirror. Experimental data: circles; same dye layers as in Figs. 28 and 29; no cover layers ($d' = 20$ Å). Theoretical plots of $\tau_M^a(d)/\tau_M^a(\infty)$ for $q = 1.0$ (solid) and $q = 0.7$ (broken) calculated with eqs. (9.21), (9.22), (9.17), (9.18) and (9.10) using for the gold mirror the optical constants $\nu = 0.505$ and $\nu\kappa = 3.66$. (From DREXHAGE [1966, 1970a].)

The experimental decay times, measured on mixed monolayers of the europium complex and tripalmitin under N_2 at 0 °C (DREXHAGE [1966]), show a less pronounced variation with the distance d than the theoretical plot of $\tau_M^a(d)/\tau_M^a(\infty)$ (Fig. 30). However, if one assumes for the quantum

* In these articles it was inadvertently omitted that the theoretical and experimental data referred to systems with both a silver mirror and a dielectric interface ($n = 1.54$; $n_1 = 1$; $d' = 0$). Likewise preliminary data, quoted by KUHN [1967] and taken on mixed layers of the europium complex and cholesterol, involved besides the metal mirror (gold) a dielectric interface ($n_1 = 1$; $d' = 0$). The theoretical curve given there was calculated by neglecting the dielectric interface, omitting the contribution described by equation (9.3) and assuming $q = 1$.

yield a value $q = 0.7$ (see section 9.4), the agreement becomes quite good. Whereas the severe discrepancies at distances between 0 and 300 Å are caused by energy transfer, the slight deviations at larger distances can be attributed possibly to the birefringence of the CdC_{20} layers, which has been neglected in the above treatment.

9.4. COMPETING NON-RADIATIVE PROCESSES

In the above discussion we have neglected any thermal deactivation processes that might occur in the excited molecule. If they are fast enough to compete with the rate of fluorescence $1/\tau$, they must be taken into account. This is usually done in terms of the quantum yield $q = L_f/(L_f+L_t)$ (equation (7.4)). If we assume that the quantity L_t is independent of the distance from the mirror, it follows that the quantum yield q_M of the molecule near the mirror is given by

$$q_M^{-1} = 1+(\tau_M/\tau)(q^{-1}-1). \tag{9.23}$$

Thus the quantity q_M varies with the distance d from the mirror. Furthermore we find for the ratio of the real decay times $\tau' = q\tau$ and $\tau'_M = q_M\tau_M$

$$\tau'/\tau'_M = 1+q[(\tau/\tau_M)-1]. \tag{9.24}$$

Hence the decay time ratios, as given by equation (9.6) etc., describe only those cases in which the thermal deactivation can be neglected ($q = 1$). If the quantity q has a value smaller than one, the variation of the decay time with distance is less pronounced, as shown for $q = 0.7$ in Fig. 30 (DREXHAGE [1970a]).

This effect can be utilized to determine the quantum yield q of the emitting state, provided that a reliable theory for τ_M exists (DREXHAGE, FLECK, KUHN, SCHÄFER, SPERLING [1966], DREXHAGE, KUHN, SCHÄFER [1968]). The method is much more sensitive than the determination of q from the critical distance of energy transfer (equation (7.5)). While, e.g., the curves of τ'_M/τ' are distinctly different for $q = 1$ and 0.7 (Fig. 30), the value of the critical distance d_0 is reduced only by the factor $0.7^{\frac{1}{6}} = 0.91$ in case of $q = 0.7$, which is within the limits of experimental error.

Appendix: Some Optical Properties of Uniaxial Crystals

The strong birefringence of the CdC_{20} layers has a distinct influence on most optical phenomena studied with these layer systems, which behave like a uniaxial crystal with the optic axis parallel to the layer normal. The angles α for the wave normal and β for the ray, being identical in isotropic

media, must be distinguished here for light polarized parallel to the plane of incidence (the extraordinary wave)*. They are related with the indices n_o and n_e by

$$n_o^2 \tan \alpha = n_e^2 \tan \beta, \tag{A.1}$$

i.e. the angle of incidence β of the ray is smaller than the corresponding angle α in case of CdC_{20} layers ($n_e > n_o$). Likewise we must distinguish between the velocity of light propagation along the wave normal and along the direction of energy flow (the ray), which may be expressed in terms of the indices n and s.

The refractive index n for the wave is given by

$$n^{-2} = n_o^{-2} \cos^2 \alpha + n_e^{-2} \sin^2 \alpha, \tag{A.2}$$

and the ray index s is related to the angle β of the ray by

$$s^2 = n_o^2 \cos^2 \beta + n_e^2 \sin^2 \beta. \tag{A.3}$$

The refraction between the layer system and an isotropic medium with refractive index n_1 (angle of incidence θ) is governed by Snell's law

$$n \sin \alpha = n_1 \sin \theta, \tag{A.4}$$

which can also be expressed as

$$n_e^2 \sin \beta = n_1 s \sin \theta. \tag{A.5}$$

The ray index s can be eliminated with equation (A.3), and one obtains relations describing the refraction of the ray:

$$\sin \beta = n_o n_1 \sin \theta / [n_e^4 + (n_o^2 - n_e^2) n_1^2 \sin^2 \theta]^{\frac{1}{2}}; \tag{A.6}$$

$$\sin \theta = n_e^2 \sin \beta / n_1 [n_o^2 + (n_e^2 - n_o^2) \sin^2 \beta]^{\frac{1}{2}}. \tag{A.7}$$

Because the electric field of the light wave is perpendicular to the ray direction (and not to the wave normal), it is often preferable to trace the rays, in particular, if one deals with absorption or emission by electric-dipole oscillators.

The reflection of light at the interface between birefringent materials has been treated by SZIVESSY [1928] p. 715 in the most general form. It can be shown that his rather complicated formulas agree with Fresnel's formulas, if one introduces the ray index s and the angle of incidence β of the ray.

* For the theory of light propagation in anisotropic media the reader is referred to the article by RAMACHANDRAN and RAMASESHAN [1961] p. 54. A very useful account, which emphasizes graphical representations, is found in the book by WAHLSTROM [1969] p. 197.

Thus one obtains for the reflection coefficients r'_{12}, r''_{21} and the transmission coefficients t''_{12}, t''_{21} at the surface of the layers

$$r''_{12} = (n_1 \cos\beta - s\cos\theta)/(n_1\cos\beta + s\cos\theta), \tag{A.8}$$

$$r''_{21} = (s\cos\theta - n_1\cos\beta)/(s\cos\theta + n_1\cos\beta), \tag{A.9}$$

$$t'_{12} = 2n_1\cos\theta/(n_1\cos\beta + s\cos\theta) \tag{A.10}$$

and

$$t'_{21} = 2s\cos\beta/(s\cos\theta + n_1\cos\beta). \tag{A.11}$$

From equations (A.8), (A.3) and (A.6) one finds for the Brewster-angle θ_{Br} ($r''_{12} = 0$)

$$\tan\theta_{Br} = (n_e/n_1)[(n_o^2 - n_1^2)/(n_e^2 - n_1^2)]^{\frac{1}{2}}. \tag{A.12}$$

With the values $n_o = 1.52$, $n_e = 1.59$ and $n_1 = 1$, e.g., it is calculated $\theta_{Br} = 55.8°$, which also would be found, if the layers were isotropic with an index $n = 1.47$. The Brewster-angle β_{Br} on the side of the layer system is found similarly:

$$\tan\beta_{Br} = (n_1/n_e)[(n_o^2 - n_1^2)/(n_e^2 - n_1^2)]^{\frac{1}{2}}. \tag{A.13}$$

With $n_o = 1.52$, $n_e = 1.59$ and $n_1 = 1$ it follows $\beta_{Br} = 30.2°$, which would be obtained in case of isotropic layers of index $n = 1.72$. It may be noted here that the direction of a ray reflected at the angle θ_{Br} is not perpendicular to the direction of the refracted ray nor to the normal of the refracted wave, nor to the electric polarization of the uniaxial medium. This casts some doubt on the validity of the common intuitive derivation of the Brewster-angle, as suggestive it may be (see, e.g., SOMMERFELD [1954] p. 25, BORN and WOLF [1970] p. 43).

In case of $n_1 > n_e$ the critical angle θ_{cr} of total reflection is given by

$$\sin\theta_{cr} = n_e/n_1, \tag{A.14}$$

whereas in the opposite case $n_1 < n_o$, n_e the critical angle β_{cr} is found from equation (A.6) as

$$\sin\beta_{cr} = n_o n_1/[n_e^4 + (n_o^2 - n_e^2)n_1^2]^{\frac{1}{2}}. \tag{A.15}$$

For instance, with the values $n_o = 1.52$, $n_e = 1.59$ and $n_1 = 1$ we calculate $\beta_{cr} = 37.7°$, a value also obtained, if the layers were isotropic with an index $n = 1.63$. This and the examples given above show that it is of questionable value to simplify the treatment of birefringent layers by assuming them to be isotropic with some average refractive index n. Equation (A.9) can be extended to the case of an *absorbing* medium 1 in the usual manner (BORN and WOLF [1970] p. 615), and thus the reflection coefficient $\rho_{\parallel}$ and the

phase shift $\delta_{\|}$ are obtained for reflection at an underlying metal mirror (section 8.4).

The radiation of an electric dipole is also influenced by its anisotropic environment. If, e.g., the dipole axis is oriented parallel to the optic axis of the layers, the electric field E_D in the far zone ($r \gg \lambda$) is given by KUEHL [1962] as

$$E_D = (4\pi^2\mu_0/\lambda^2 r)(n_o n_e^2/s^3) \sin\beta, \tag{A.16}$$

and the total energy L_f, emitted by the oscillator per unit time, is obtained in analogy to section 9.1:

$$L_f = \frac{c}{8\pi}\int_0^{\pi}\int_0^{2\pi} sE_D^2 r^2 \sin\beta \, d\beta \, d\psi = 16\pi^4 c n_o \mu_0^2/3\lambda^4. \tag{A.17}$$

The total radiation field of an electric dipole, including the near zone, has been derived by CLEMMOW [1966] p. 159.

Acknowledgments

The author expresses his gratitude for the cooperation and support which he has received from many colleagues at the University of Marburg during the course of his work there. In particular, I wish to thank Prof. H. Kuhn and F. P. Schäfer for many stimulating discussions and helpful suggestions. I am also grateful to Prof. H. Wolter, whose excellent lectures have inspired my interest in optics. The valuable suggestions regarding the manuscript by H. Bücher and F. C. Strome Jr. of the Eastman Kodak Laboratories are greatly appreciated.

References

AUGENSTINE, L. G., 1960, in: Comparative Effects of Radiation, Conf. Proc., Puerto Rico 1960, eds. M. Burton, J. S. Kirby-Smith and J. L. Magee (John Wiley, New York) p. 322.

BARTH, P., K. H. BECK, K. H. DREXHAGE, H. KUHN, D. MÖBIUS, D. MOLZAHN, K. RÖLLIG, F. P. SCHÄFER, W. SPERLING and M. M. ZWICK, 1966, Optische und elektrische Phänomene an monomolekularen Farbstoffschichten, in: Optische Anregung organischer Systeme, Conf. Proc., Schloss Elmau 1964, ed. W. Foerst (Verlag Chemie, Weinheim/Bergstr.) p. 639.

BAUER, H., J. BLANC and D. L. ROSS, 1964, J. Amer. Chem. Soc. **86**, 5125.

BERNSTEIN, S., 1940, J. Amer. Chem. Soc. **62**, 374.

BLODGETT, Katharine B., 1934, J. Amer. Chem. Soc. **56**, 495.

BLODGETT, Katharine B., 1935, J. Amer. Chem. Soc. **57**, 1007.

BLODGETT, Katharine B. and I. LANGMUIR, 1937, Phys. Rev. **51**, 964.

BLODGETT, Katharine B., 1939, Phys. Rev. **55**, 391.

BORN, M. and E. WOLF, 1970, Principles of Optics, 4th ed. (Pergamon Press, Oxford).

BÜCHER, H., K. H. DREXHAGE, M. FLECK, H. KUHN, D. MÖBIUS, F. P. SCHÄFER, J. SONDERMANN, W. SPERLING, P. TILLMANN and J. WIEGAND, 1967, Mol. Cryst. **2**, 199.
BÜCHER, H., H. KUHN, B. MANN, D. MÖBIUS, L. v. SZENTPÁLY and P. TILLMANN, 1967, Photogr. Sci. Eng. **11**, 233.
BÜCHER, H., O. v. ELSNER, D. MÖBIUS, P. TILLMANN and J. WIEGAND, 1969, Z. Phys. Chem. (Frankfurt am Main) **65**, 152.
BÜCHER, H., J. WIEGAND, B. B. SNAVELY, K. H. BECK and H. KUHN, 1969, Chem. Phys. Letters **3**, 508.
BÜCHER, H., 1970, Dissertation, University of Marburg, Germany.
BÜCHER, H. and H. KUHN, 1970, Z. Naturforsch. B **25**, 1323.
CARNIGLIA, C. K., L. MANDEL and K. H. DREXHAGE, 1972, J. Opt. Soc. Amer. **62**, 479.
CLEMMOW, P. C., 1966, The Plane Wave Spectrum Representation of Electromagnetic Fields (Pergamon Press, Oxford).
DEXTER, D. L., 1953, J. Chem. Phys. **21**, 836.
DOERMANN, F. W., 1938, Phys. Rev. **53**, 420.
DOERMANN, F. W. and O. HALPERN, 1939, Phys. Rev. **55**, 486.
DREXHAGE, K. H., M. M. ZWICK and H. KUHN, 1963, Ber. Bunsenges. Phys. Chem. **67**, 62.
DREXHAGE, K. H., 1964, Dissertation, University of Marburg, Germany.
DREXHAGE, K. H., 1966, Optische Untersuchungen an neuartigen monomolekularen Farbstoffschichten (Habilitations-Schrift, University of Marburg, Germany).
DREXHAGE, K. H., M. FLECK, H. KUHN, F. P. SCHÄFER and W. SPERLING, 1966, Ber. Bunsenges. Phys. Chem. **70**, 1179.
DREXHAGE, K. H. and H. KUHN, 1966, Optical and Electrical Phenomena on Monomolecular Layers, in: Basic Problems in Thin Film Physics, Conf. Proc., Clausthal-Göttingen 1965, eds. R. Niedermayer and H. Mayer (Vandenhoeck-Ruprecht, Göttingen) p. 339.
DREXHAGE, K. H., M. FLECK and H. KUHN, 1967, Ber. Bunsenges. Phys. Chem. **71**, 915.
DREXHAGE, K. H. and H. FORSTER, 1967, Quantitative Untersuchung der bei der Totalreflexion am optisch dünneren Medium auftretenden Grenzflächenwelle, paper presented at the Westdeutsche Chemiedozententagung, Saarbrücken, Germany, April 12.
DREXHAGE, K. H., H. KUHN and F. P. SCHÄFER, 1968, Ber. Bunsenges. Phys. Chem. **72**, 329.
DREXHAGE, K. H. and M. FLECK, 1968, Ber. Bunsenges. Phys. Chem. **72**, 330.
DREXHAGE, K. H., 1969, Long Range Energy Transfer Involving Higher Order Transitions, paper presented at the Fifth Intern. Conf. on Photochemistry, Yorktown Heights, New York, September 2.
DREXHAGE, K. H., 1970a, J. Luminesc. **1, 2**, 693.
DREXHAGE, K. H., 1970b, Scientific American **222**, 108.
DREXHAGE, K. H., 1972, Spontaneous Emission Rate in the Presence of a Mirror, Third Rochester Conf. on Coherence and Quantum Optics, Rochester, New York, June 21.
DREXHAGE, K. H., 1974, Photogr. Sci. Eng. (to be published).
DRUDE, P. and W. NERNST, 1892, Wiedem. Ann. Phys. u. Chem. **45**, 460.
ELSNER, O. v., 1969, Dissertation, University of Marburg, Germany.
ENGELSEN, D. DEN, 1971, J. Opt. Soc. Amer. **61**, 1460.
ENGELSEN, D. DEN, 1972, J. Phys. Chem. **76**, 3390.
FLECK, M., 1969, Dissertation, University of Marburg, Germany.
FÖRSTER, T., 1946, Naturwissenschaften **33**, 166.
FÖRSTER, T., 1948, Ann. Phys., 6. Folge **2**, 55.
FORSTER, H., 1967, Diplomarbeit, University of Marburg, Germany.
FREED, S. and S. I. WEISSMAN, 1941, Phys. Rev. **60**, 440.
GAINES Jr., G. L., 1966, Insoluble Monolayers at Liquid-Gas Interfaces (Interscience, New York).
HALPERN, O. and F. W. DOERMANN, 1937, Phys. Rev. **52**, 937.
HAUGLAND, R. P., J. YGUERABIDE and L. STRYER, 1969, Proc. Nat. Acad. Sci. U.S. **63**, 23.

HOLLEY, C., 1938, Phys. Rev. **53**, 534.
INACKER, O., H. KUHN, H. BÜCHER, H. MEYER and K. H. TEWS, 1970, Chem. Phys. Letters **7**, 213.
KAUZMANN, W., 1957, Quantum Chemistry (Academic Press, New York).
KLEUSER, D. and H. BÜCHER, 1969, Z. Naturforsch. B **24**, 1371.
KOPPELMANN, G., 1969, Multiple-Beam Interference and Natural Modes in Open Resonators, *in*: Progress in Optics, Vol. 7, ed. E. Wolf (North-Holland, Amsterdam) p. 1.
KOSSEL, D., 1958, Praxis der Naturwissenschaften **7**, 44.
KUEHL, H. H., 1962, Phys. Fluids **5**, 1095.
KUHN, H., 1967, Naturwissenschaften **54**, 429.
KUHN, H., 1968, On Possible Ways of Assembling Simple Organized Systems of Molecules, in: Structural Chemistry and Molecular Biology, eds. A. Rich and N. Davidson (W. H. Freeman, San Francisco) p. 566.
KUHN, H., 1970, J. Chem. Phys. **53**, 101.
KUHN, H. and D. MÖBIUS, 1971, Angew. Chem. **83**, 672; internat. Edit. **10**, 620.
KUHN, H., 1972, Spectroscopy of Monolayer Assemblies, Part I, Principles and Applications, in: Physical Methods of Chemistry, Part IIIB, eds. A. Weissberger and B. W. Rossiter (Wiley-Interscience, New York) p. 579.
KUHN, W., 1933, Theorie und Grundgesetze der optischen Aktivität, in: Stereochemie, ed. K. Freudenberg (F. Deuticke, Leipzig) p. 317.
MANN, B., H. KUHN and L. v. SZENTPÁLY, 1971, Chem. Phys. Letters **8**, 82.
MAYER, H., 1950, Physik dünner Schichten, Part I (Wiss. Verlagsges., Stuttgart).
MÖBIUS, D., 1969, Z. Naturforsch. A **24**, 251.
MÖBIUS, D. and H. BÜCHER, 1972, Spectroscopy of Monolayer Assemblies, Part II, Experimental Procedure, in: Physical Methods of Chemistry, Part IIIB, eds. A. Weissberger and B. W. Rossiter (Wiley-Interscience, New York) p. 650.
MORAWITZ, H., 1969, Phys. Rev. **187**, 1792.
RAMACHANDRAN, G. N. and S. RAMASESHAN, 1961, Crystal Optics, in: Handbuch der Physik, Vol. 25/1, ed. S. Flügge (Springer, Berlin) p. 1.
ROTHEN, A., 1945, Rev. Sci. Instrum. **16**, 26.
ROTHEN, A., 1968, Surface Film Techniques, in: Physical Techniques in Biological Research, 2nd ed., Vol. 2, Part A, ed. D. H. Moore (Academic Press, New York) p. 217.
SCHAEFER, C. and G. GROSS, 1910, Ann. Phys., 4. Folge **32**, 648.
SCHMIDT, S., R. REICH and H. T. WITT, 1969, Z. Naturforsch. B **24**, 1428.
SCHMIDT, S., R. REICH and H. T. WITT, 1971, Naturwissenschaften **58**, 414.
SCHMIDT, S. and R. REICH, 1972a, Ber. Bunsenges. Phys. Chem. **76**, 599.
SCHMIDT, S. and R. REICH, 1972b, Ber. Bunsenges. Phys. Chem. **76**, 1202.
SELÉNYI, P., 1911, Ann. Phys., 4. Folge **35**, 444.
SELÉNYI, P., 1913, C. R. Acad. Sci. **157**, 1408.
SELÉNYI, P., 1938, Z. Physik **108**, 401.
SELÉNYI, P., 1939, Phys. Rev. **56**, 477.
SHER, I. H. and J. D. CHANLEY, 1955, Rev. Sci. Instrum. **26**, 266.
SHKLYAREVSKII, I. N., V. K. MILOSLAVSKII and V. I. GOLOYADOVA, 1964, Opt. Spectrosc. **17**, 413; Russ.: **17** (1964) 765.
SOMMERFELD, A., 1954, Optics (Academic Press, New York).
SONDERMANN, J., 1971, Liebigs Ann. Chem. **749**, 183.
STEIGER, R., 1971, Helv. Chim. Acta **54**, 2645.
STRYER, L. and R. P. HAUGLAND, 1967, Proc. Nat. Acad. Sci. U.S. **58**, 719.
SZENTPÁLY, L. v., D. MÖBIUS and H. KUHN, 1970, J. Chem. Phys. **52**, 4618.
SZIVESSY, G., 1928, Kristalloptik, in: Handbuch der Physik, Vol. 20, eds. H. Geiger and K. Scheel (Springer, Berlin) p. 635.
TEWS, K. H., O. INACKER and H. KUHN, 1970, Nature (London) **228**, 276; erratum: **228**, 791.

TILLMANN, P., 1966, Dissertation, University of Marburg, Germany.
TRURNIT, H. J., 1945, Über monomolekulare Filme an Wassergrenzflächen und über Schichtfilme, in: Fortschritte der Chemie organischer Naturstoffe, Vol. 4, ed. L. Zechmeister (Springer, Berlin) p. 347.
WAHLSTROM, E. E., 1969, Optical Crystallography, 4th ed. (John Wiley, New York).
WIENER, O., 1890, Wiedem. Ann. Phys. u. Chem. **40**, 203.
WOLTER, H., 1956, Optik dünner Schichten, in: Handbuch der Physik, Vol. 24, ed. S. Flügge (Springer, Berlin) p. 461.
WOOD, R. W., 1934, Physical Optics, 3rd ed. (Macmillan, New York).
ZWICK, M. M. and H. KUHN, 1962, Z. Naturforsch. A **17**, 411.